

ACTIVE FEW-SHOT FINE-TUNING

Jonas Hübötter*, Bhavya Sukhija, Lenart Treven, Yarden As, Andreas Krause
ETH Zurich, Switzerland

ABSTRACT

We study the question: *How can we select the right data for fine-tuning to a specific task?* We call this data selection problem *active fine-tuning* and show that it is an instance of transductive active learning, a novel generalization of classical active learning. We propose **ITL**, short for *information-based transductive learning*, an approach which samples adaptively to maximize information gained about the specified task. We are the first to show, under general regularity assumptions, that such decision rules converge uniformly to the smallest possible uncertainty obtainable from the accessible data. We apply **ITL** to the few-shot fine-tuning of large neural networks and show that fine-tuning with **ITL** learns the task with significantly *fewer* examples than the state-of-the-art.

1 INTRODUCTION

Despite the remarkable successes of large neural networks (NNs) across various fields, such as image classification and natural language processing, their performance can deteriorate when faced with slight variations between the source and target domains (Recht et al., 2019; Hendrycks & Dietterich, 2019; Koh et al., 2021; Lee et al., 2022). Additionally, training large NNs requires large amounts of (labeled) data, which is often expensive or even impossible to obtain, and furthermore, training on such large datasets requires prohibitive computational resources.

Fine-tuning a large pre-trained model on a (small) dataset from the target domain is a cost- and computation-effective approach to address the distribution shift between source and target domains. While previous work has studied the effectiveness of various training procedures for fine-tuning (Howard & Ruder, 2018; Kornblith et al., 2019; Shen et al., 2021; Lee et al., 2022; Silva-Rodríguez et al., 2023), the problem of obtaining a good dataset for fine-tuning has received less attention. Selecting such a *small* dataset is challenging, as it requires selecting the most relevant and diverse data from a large dataset based only on a few reference examples from the target domain.

In this work, we propose a generalization of classical active learning, *transductive active learning*. We show that the fine-tuning of large neural networks can be seen as transductive active learning, and propose **ITL** which significantly improves upon the state-of-the-art — *enabling efficient few-shot fine-tuning of large neural networks*.

Transductive active learning We consider the problem of *transductive active learning*, where provided an unknown and sufficiently regular function f over a domain \mathcal{X} and given two arbitrary subsets of the domain; a *target space* $\mathcal{A} \subseteq \mathcal{X}$, and a *sample space* $\mathcal{S} \subseteq \mathcal{X}$, we study the question:

*How can we learn f within \mathcal{A}
by actively sampling observations within \mathcal{S} ?*

Prior work on active learning commonly aims to learn f globally, i.e., across the entire domain \mathcal{X} . However, in many real-world problems, (i) the domain \mathcal{X} is so large

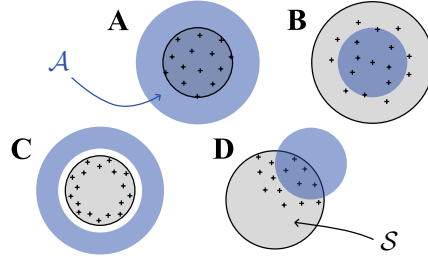


Figure 1: Instances of transductive active learning where the target space \mathcal{A} is shown in blue and the sample space \mathcal{S} is shown in gray. The points denote plausible observations within \mathcal{S} to “learn” \mathcal{A} . In (A), the target space contains “everything” within \mathcal{S} as well as points *outside* \mathcal{S} . In (B, C, D), one makes observations *directed* towards learning about a particular target. Prior work on active learning has focused on the instances $\mathcal{A} = \mathcal{S}$ and $\mathcal{A} \subset \mathcal{S}$.

*Correspondence to jonas.huebottter@inf.ethz.ch

that learning f globally is hopeless or **(ii)** agents have limited information and cannot access the entire domain \mathcal{X} (e.g., due to restricted access or to act safely). Thus, global learning is often not desirable or even possible. Instead, intelligent systems are typically required to act in a more *directed* manner and *extrapolate* beyond their limited information. This work studies the above two aspects of active learning, which have remained largely unaddressed by prior work. We provide a comprehensive overview of related work in Section 5.

The fine-tuning of large neural networks is an instance of transductive active learning, where the target space \mathcal{A} represents the test set over which we want to minimize risk, and the sample space \mathcal{S} represents the dataset from which we can retrieve data points to fine-tune our model to \mathcal{A} . Figure 1 visualizes some instances of transductive active learning. Whereas most prior work has focused on the instance $\mathcal{X} = \mathcal{A} = \mathcal{S}$, MacKay (1992) was the first to consider specific target spaces \mathcal{A} as in (B), and transductive active learning generalizes to other instances such as (A), (C), and (D).

Contributions

- We are the first to give rates for the uniform convergence of uncertainty over the target space \mathcal{A} to the smallest attainable value, given samples from the sample space \mathcal{S} (Theorem 3.1), which implies a new generalization bound for functions in reproducing kernel Hilbert spaces (Theorem 3.2).
- We apply the transductive active learning framework to batch-wise *active few-shot fine-tuning of large neural networks* and show empirically that **ITL** substantially outperforms the state-of-the-art (Section 4).

2 PRELIMINARIES

We assume that the target space \mathcal{A} and sample space \mathcal{S} are finite.¹ We model f as a stochastic process and denote the marginal random variables $f(x)$ by f_x , and joint random vectors $\{f(x)\}_{x \in X}$ for some $X \subseteq \mathcal{X}$, $|X| < \infty$ by \mathbf{f}_X . Let \mathbf{y}_X denote the noisy observations of \mathbf{f}_X , $\{y_x = f_x + \varepsilon_x\}_{x \in X}$, where ε_x is independent noise.² We study the “adaptive” setting, where in round n the agent selects a point $x_n \in \mathcal{S}$ and observes $y_n = y_{x_n}$. The agent’s choice of x_n may depend on the prior observations $\mathcal{D}_{n-1} \stackrel{\text{def}}{=} \{(x_i, y_i)\}_{i < n}$.

Background on information theory We briefly recap several important concepts from information theory, of which we provide formal definitions in Appendix B. The (differential) entropy $H[\mathbf{f}]$ is a measure of uncertainty about \mathbf{f} and the conditional entropy $H[\mathbf{f} | \mathbf{y}]$ is the (expected) posterior uncertainty about \mathbf{f} after observing \mathbf{y} . The information gain $I(\mathbf{f}; \mathbf{y}) = H[\mathbf{f}] - H[\mathbf{f} | \mathbf{y}]$ measures the (expected) reduction in uncertainty about \mathbf{f} due to \mathbf{y} . The maximum information gain from n noisy observations within \mathcal{S} is

$$\gamma_n \stackrel{\text{def}}{=} \max_{\substack{X \subseteq \mathcal{S} \\ |X| \leq n}} I(\mathbf{f}_X; \mathbf{y}_X).$$

This has been used previously (e.g., by Srinivas et al., 2009; Chowdhury & Gopalan, 2017; Vakili et al., 2021) as a measure of the “information capacity” of f .

3 MAIN RESULTS ON TRANSDUCTIVE ACTIVE LEARNING

We propose **ITL**, which greedily maximizes the information gain at each round n between the prediction targets $\mathbf{f}_\mathcal{A}$ and the observation y_x conditioned on the prior observations \mathcal{D}_{n-1} . Formally,

$$x_n = \arg \max_{x \in \mathcal{S}} I(\mathbf{f}_\mathcal{A}; y_x | \mathcal{D}_{n-1}). \quad (\text{ITL})$$

This simple decision rule generalizes several widely used algorithms which we discuss in more detail in Section 5.

¹Infinite domains can be addressed via discretization arguments from the Bayesian optimization literature.

² X may be a multiset, in which case repeated x correspond to repeated independent observations of y_x .

We also consider an additional correlation-based decision rule, which will later uncover connections to existing approaches:

$$\mathbf{x}_n = \arg \max_{\mathbf{x} \in \mathcal{S}} \sum_{\mathbf{x}' \in \mathcal{A}} \text{Cor}[f_{\mathbf{x}}, f_{\mathbf{x}'} \mid \mathcal{D}_{n-1}]. \quad (\mathbf{CTL})$$

Unlike **CTL**, **ITL** takes into account the mutual dependence between points in \mathcal{A} .

In the following Sections 3.1 and 3.2, we discuss general settings in which the convergence properties of **ITL** can be analyzed theoretically.

3.1 GAUSSIAN PROCESS SETTING

When $f \sim \mathcal{GP}(\mu, k)$ is a Gaussian process (GP, Williams & Rasmussen (2006)) with known mean function μ and kernel k , and the noise $\varepsilon_{\mathbf{x}}$ is mutually independent and zero-mean Gaussian with known variance $\rho^2(\mathbf{x}) > 0$, the **ITL** objective has a closed form expression:

$$\mathbf{I}(\mathbf{f}_{\mathcal{A}}; y_{\mathbf{x}} \mid \mathcal{D}_{n-1}) = \frac{1}{2} \log \left(\frac{\text{Var}[y_{\mathbf{x}} \mid \mathcal{D}_{n-1}]}{\text{Var}[y_{\mathbf{x}} \mid \mathbf{f}_{\mathcal{A}}, \mathcal{D}_{n-1}]} \right). \quad (1)$$

Further, the information capacity γ_n is sublinear in n for a rich class of GPs, with rates summarized in Table 3 of the appendix (Srinivas et al., 2009; Vakili et al., 2021).

Convergence to irreducible uncertainty So far, our discussion was centered around the role of the target space \mathcal{A} in facilitating *directed* learning. An orthogonal contribution of this work is to study *extrapolation* from the sample space \mathcal{S} to points $\mathbf{x} \in \mathcal{A} \setminus \mathcal{S}$. To this end, we derive bounds on the marginal posterior variance $\sigma_n^2(\mathbf{x}) \stackrel{\text{def}}{=} \text{Var}[f(\mathbf{x}) \mid \mathcal{D}_n]$ for points in \mathcal{A} . For ease of presentation, we assume in the following that $\mathcal{S} \subseteq \mathcal{A}$, however, the results are straightforward to generalize to other instances (Hübotter et al., 2024). For **ITL**, these bounds imply uniform convergence of the variance for a rich class of GPs. To the best of our knowledge, we are the first to derive such bounds, and they might be of independent interest for active learning.

We define the *irreducible uncertainty* as the variance of $f(\mathbf{x})$ provided complete knowledge of f in \mathcal{S} :

$$\eta_{\mathcal{S}}^2(\mathbf{x}) \stackrel{\text{def}}{=} \text{Var}[f_{\mathbf{x}} \mid \mathbf{f}_{\mathcal{S}}].$$

As the name suggests, $\eta_{\mathcal{S}}^2(\mathbf{x})$ represents the smallest uncertainty one can hope to achieve from observing only within \mathcal{S} . For all $\mathbf{x} \in \mathcal{S}$, it is easy to see that $\eta_{\mathcal{S}}^2(\mathbf{x}) = 0$. However, the irreducible uncertainty of $\mathbf{x} \notin \mathcal{S}$ may be (and typically is!) strictly positive.

Theorem 3.1 (Generalization bound on marginal variance for **ITL**). *Assume that $f \sim \mathcal{GP}(\mu, k)$ with known mean function μ and kernel k , the noise $\varepsilon_{\mathbf{x}}$ is mutually independent and zero-mean Gaussian with known variance $\rho^2(\mathbf{x}) > 0$, and γ_n is sublinear in n . Then, for any $n \geq 1, \epsilon > 0$, and $\mathbf{x} \in \mathcal{A}$, there exists a constant C such that*

$$\sigma_n^2(\mathbf{x}) \leq \underbrace{\eta_{\mathcal{S}}^2(\mathbf{x})}_{\text{irreducible}} + \underbrace{C\gamma_n/\sqrt{n}}_{\text{reducible}}. \quad (2)$$

Intuitively, Equation (2) of Theorem 3.1 can be understood as bounding an epistemic “generalization gap” (Wainwright, 2019) of the learner. The reducible uncertainty converges to zero, e.g., for Gaussian and smooth Matérn kernels, at all prediction targets $\mathbf{x} \in \mathcal{A}$. We provide a formal proof of Theorem 3.1 in Appendix D.3.

3.2 AGNOSTIC SETTING

The result from the GP setting translates also to the agnostic setting, where the “ground truth” f^* may be any sufficiently regular fixed function on \mathcal{X} .³ In this case, we use the model f from Section 3.1 as a (misspecified) model of f^* , with some kernel k and zero mean function $\mu(\cdot) = 0$. We denote by $\mu_n(\mathbf{x}) \stackrel{\text{def}}{=} \mathbb{E}[f(\mathbf{x}) \mid \mathcal{D}_n]$ the posterior mean of f . W.l.o.g. we assume in the following result that the prior variance is bounded, i.e., $\text{Var}[f(\mathbf{x})] \leq 1$.⁴

³Here $f^*(\mathbf{x})$ denotes the mean observation $y_{\mathbf{x}} = f^*(\mathbf{x}) + \epsilon_{\mathbf{x}}$

⁴The results can be generalized to kernels with $\text{Var}[f(\mathbf{x})] \leq c$ (Chowdhury & Gopalan, 2017).

Theorem 3.2 (Bound on generalization error for **ITL**, following Abbasi-Yadkori (2013); Chowdhury & Gopalan (2017)). *Pick any $\delta \in (0, 1)$. Assume that f^* lies in the reproducing kernel Hilbert space $\mathcal{H}_k(\mathcal{X})$ of the kernel k with norm $\|f^*\|_k < \infty$, the noise ε_n is conditionally ρ -sub-Gaussian, and γ_n is sublinear in n . Let $\beta_n(\delta) = \|f^*\|_k + \rho\sqrt{2(\gamma_n + 1 + \log(1/\delta))}$. Then, for any $n \geq 1$ and $\mathbf{x} \in \mathcal{A}$, jointly with probability at least $1 - \delta$,*

$$|f^*(\mathbf{x}) - \mu_n(\mathbf{x})| \leq \beta_n(\delta) \left[\underbrace{\eta_{\mathcal{S}}(\mathbf{x})}_{\text{irreducible}} + \underbrace{\nu(n)}_{\text{reducible}} \right]$$

where $\nu^2(n)$ denotes the reducible part of Equation (2).

We provide a formal proof of Theorem 3.2 in Appendix D.4. Theorem 3.2 generalizes confidence bounds of prior works to the extrapolation setting, where some prediction targets $\mathbf{x} \in \mathcal{A}$ lie outside the sample space \mathcal{S} . Theorem 3.2 can therefore be interpreted as a *generalization bound* which holds uniformly for all functions f^* with $\|f^*\|_k < \infty$. For prediction targets $\mathbf{x} \in \mathcal{A} \cap \mathcal{S}$, the irreducible uncertainty vanishes, and we recover previous results from the setting $\mathcal{S} = \mathcal{A}$.

Theorems 3.1 and 3.2 show that **ITL** efficiently learns f at the prediction targets \mathcal{A} for large classes of “sufficiently regular” functions f . In the following, we validate these results experimentally by showing that **ITL** exhibits strong empirical performance for fine-tuning large neural networks.

4 FEW-SHOT FINE-TUNING OF NEURAL NETWORKS

As discussed in Section 1, the fine-tuning of large neural networks to downstream tasks can be framed as a transductive active learning problem. In our experiments, we consider a supervised learning problem, where the function f maps inputs $\mathbf{x} \in \mathcal{X}$ to outputs $y \in \mathcal{Y}$.⁵ We have access to noisy samples from a training set \mathcal{S} on \mathcal{X} , and we would like to learn f such that our estimate minimizes a given risk measure, such as classification error, with respect to a test distribution $\mathcal{P}_{\mathcal{A}}$ on \mathcal{X} . Ideally, $\mathcal{P}_{\mathcal{S}}$ and $\mathcal{P}_{\mathcal{A}}$ are identical, however, in many real-world cases $\mathcal{P}_{\mathcal{S}}$ differs substantially from $\mathcal{P}_{\mathcal{A}}$. This is for instance the case when samples from $\mathcal{P}_{\mathcal{A}}$ are expensive to obtain, such as in medical imaging. The goal is to actively and efficiently sample from \mathcal{S} to minimize risk with respect to $\mathcal{P}_{\mathcal{A}}$.⁶ We show in this section that **ITL** can learn f from only *few examples* from \mathcal{S} .

How can we leverage the latent structure learned by the pre-trained model? As common in related work, we approximate the (pre-trained) neural network (NN) $f(\cdot; \theta)$ as a linear function in a latent embedding space, $f(\mathbf{x}; \theta) \approx \beta^\top \phi_\theta(\mathbf{x})$, with weights $\beta \in \mathbb{R}^p$ and embeddings $\phi_\theta : \mathcal{X} \rightarrow \mathbb{R}^p$. Common choices of embeddings include last-layer embeddings (Devlin et al., 2019; Holzmüller et al., 2023), neural tangent embeddings arising from neural tangent kernels (Jacot et al., 2018) which are motivated by their relationship to the training and fine-tuning of ultra-wide NNs (Arora et al., 2019; Lee et al., 2019; Khan et al., 2019; He et al., 2020; Malladi et al., 2023), and loss gradient embeddings (Ash et al., 2020). We provide a comprehensive overview of embeddings in Appendix H.2. Now, supposing the prior $\beta \sim \mathcal{N}(\mathbf{0}, \Sigma)$, often with $\Sigma = \mathbf{I}$ (Khan et al., 2019; He et al., 2020; Antorán et al., 2022; Wei et al., 2022), this approximation of f is a Gaussian process with kernel $k(\mathbf{x}, \mathbf{x}') = \phi_\theta(\mathbf{x})^\top \Sigma \phi_\theta(\mathbf{x}')$ which quantifies the similarity between points in terms of their alignment in the learned latent space. Note that the correlation $k(\mathbf{x}, \mathbf{x}') / \sqrt{k(\mathbf{x}, \mathbf{x})k(\mathbf{x}', \mathbf{x}')}$ between two points \mathbf{x}, \mathbf{x}' is equal to the cosine similarity of their embeddings.

In this context, Theorem 3.1 bounds the epistemic posterior uncertainty about a prediction using the approximation $\beta^\top \phi_\theta(\mathbf{x})$, given that the model is trained using data selected by **ITL**. Theorem 3.2 bounds the generalization error when using the posterior mean of β for prediction. This extends recent work which has studied estimators of this generalization error (Wei et al., 2022).

Batch selection: Diversity via conditional embeddings Efficient labeling and training necessitates a batch-wise selection of inputs. The selection of a batch of size $b > 1$ can be seen as an individual *non-adaptive* active learning problem, and significant recent work has shown that batch diversity is crucial in this setting (Ash et al., 2020; Zanette et al., 2021; Holzmüller et al., 2023; Pacchiano

⁵We remark that also the semi-supervised or unsupervised fine-tuning of models can be framed as a transductive active learning problem.

⁶The setting with target distributions $\mathcal{P}_{\mathcal{A}}$ can be reduced to considering target sets \mathcal{A} , cf. Appendix F.

et al., 2024). A batch-wise selection strategy is formalized by the following NP-hard non-adaptive transductive active learning problem (Krause & Golovin, 2014; Golovin & Krause, 2011):

$$B_n = \arg \max_{B \subseteq \mathcal{S}, |B|=b} I(\mathbf{f}_A; \mathbf{y}_B \mid \mathcal{D}_{n-1}). \quad (3)$$

ITL solves this optimization problem greedily:

$$\mathbf{x}_{n,i} = \arg \max_{\mathbf{x} \in \mathcal{S}} I(\mathbf{f}_A; \mathbf{y}_{\mathbf{x}} \mid \mathcal{D}_{n-1}, \mathbf{y}_{\mathbf{x}_{n,1:i-1}}). \quad (4)$$

We show in Appendix C that the approximation error of $B'_n = \mathbf{x}_{n,1:b}$ can be bounded in terms of the submodularity ratio of **ITL** (Das & Kempe, 2018). For example, if $\mathcal{S} \subseteq \mathcal{A}$, the problem from Equation (3) is submodular and the B'_n is a $(1 - 1/e)$ -approximation of B_n (Nemhauser et al., 1978; Krause & Golovin, 2014). The batch B_n , and therefore also B'_n , is diverse and informative by design. We discuss an efficient iterative implementation of Equation (4) in Appendix H.4. Prior work has shown that the greedy solution B'_n is also competitive with a fully sequential “batchless” decision rule (Chen & Krause, 2013; Esfandiari et al., 2021).⁷

4.1 EXPERIMENTS

Our empirical evaluation is motivated by the following practical example: We deploy a pre-trained image classifier to user’s phones who use it within their local environment. We would like to locally fine-tune a user’s model to their environment. Since the users’ images \mathcal{A} are unlabeled, this requires selecting a small number of relevant and diverse images from the set of labeled images \mathcal{S} . As such, we will focus here on the setting where the points in our test set do not lie in our training set (i.e., $\mathcal{A} \cap \mathcal{S} = \emptyset$), while Hübötter et al. (2024) discusses also alternative settings such as active domain adaptation.

Testbeds & architectures We use the MNIST (LeCun et al., 1998) and CIFAR-100 (Krizhevsky et al., 2009) datasets as testbeds. In both cases, we take \mathcal{S} to be the training set, and we consider the task of learning the digits 3, 6, and 9 (MNIST) or the first 10 categories of CIFAR-100.⁸ For MNIST, we train a simple convolutional neural network with ReLU activations, three convolutional layers with max-pooling, and two fully-connected layers. For CIFAR-100, we fine-tune an EfficientNet-B0 (Tan & Le, 2019) pre-trained on ImageNet (Deng et al., 2009), augmented by a final fully-connected layer. We train the NNs using the cross-entropy loss and the ADAM optimizer (Kingma & Ba, 2014).

Results In Figure 2, We compare against (i) active learning methods which largely aim for sample diversity but which are not directed towards the target distribution \mathcal{P}_A (e.g., BADGE; Ash et al., 2020), and (ii) search methods that aim to retrieve the most relevant samples from \mathcal{S} with respect to the targets \mathcal{P}_A (e.g., maximizing cosine similarity to target embeddings as is common in vector databases; Settles & Craven, 2008; Johnson et al., 2019). INFORMATIONDENSITY (ID, Settles & Craven, 2008) is a heuristic approach aiming to combine (i) diversity and (ii) relevance. We observe that **ITL** and **CTL** consistently and significantly outperform random sampling from \mathcal{S} as well as all baselines. We see that relevance-based methods such as COSINESIMILARITY have an initial advantage over RANDOM but for batch sizes larger than 1 they quickly fall behind due to diminishing informativeness of the selected data. In contrast, diversity-based methods such as BADGE are more competitive with RANDOM but do not explicitly aim to retrieve relevant samples.

In Figure 3, we compare *batch selection via conditional embeddings* (BACE) to selecting the top- b points according to the decision rule (which does *not* yield diverse batches). We observe a significant improvement in accuracy and data retrieval when using BACE. We expect the gap between both approaches to widen further with larger batch sizes.

Synthesizing sample relevance and diversity Our proposed methods synthesize approaches to coverage (promoting *diverse* samples) and search (aiming for *relevant* samples with respect to a given query \mathcal{A}) which leads to the significant improvement upon the state-of-the-art in Figure 2. Notably, for a batch size and query size of 1 and if correlations are non-negative, **ITL**, **CTL**, and the canonical cosine similarity are equivalent. **CTL** can be seen as a direct generalization of cosine

⁷They prove this for the case where Equation (3) is submodular, but their results readily generalize to “approximate” submodularity.

⁸That is, we restrict \mathcal{P}_A to the support of points with labels $\{3, 6, 9\}$ (MNIST) or labels $\{0, \dots, 9\}$ (CIFAR-100) and train a neural network using few examples drawn from the training set \mathcal{S} .

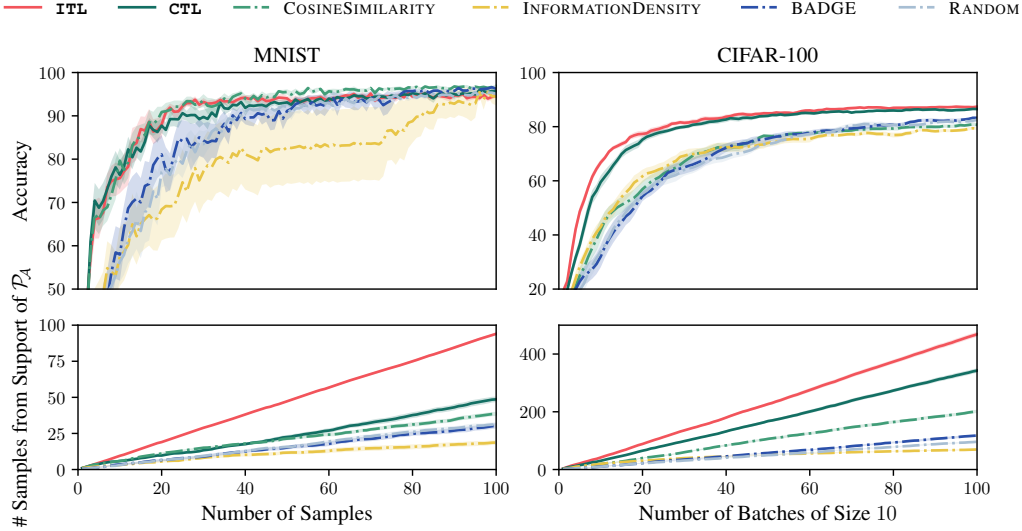


Figure 2: Few-shot training of NNs on MNIST (left) and CIFAR-100 (right). **RANDOM** selects each observation uniformly at random from \mathcal{P}_S . The batch size is 1 for MNIST and 10 for CIFAR-100. Uncertainty bands correspond to one standard error over 10 random seeds. We see that **ITL** significantly outperforms the state-of-the-art, and in particular, retrieves substantially more samples from the support of \mathcal{P}_A than competing methods. This trend becomes even more pronounced in more difficult large-scale learning tasks (cf. Figure 7 in Appendix H). See Appendix H for details and additional experiments.

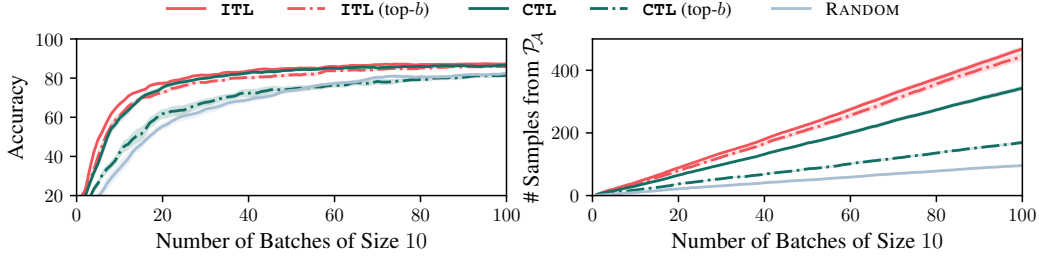


Figure 3: Batch selection via conditional embeddings improves substantially over selecting the top- b candidates proposed by the decision rule. This is the CIFAR-100 experiment (where $b = 10$).

similarity-based retrieval to batch and query sizes larger than one. In contrast to **CTL**, **ITL** may also sample points which exhibit a strong negative correlation (which is also informative).

We observe empirically that **ITL** obtains samples from \mathcal{P}_A at more than twice the rate of **COSINESIMILARITY**, which translates to a significant improvement in accuracy in more difficult learning tasks, while requiring fewer (labeled) samples from \mathcal{S} . This phenomenon manifests for both MNIST and CIFAR-100, as well as imbalanced datasets \mathcal{S} or imbalanced reference samples from \mathcal{P}_A (cf. Appendix H.6). The improvement in accuracy appears to increase in the large-data regime, where the learning tasks become more difficult. Akin to a previously identified scaling trend with size of the pre-training dataset (Tamkin et al., 2022), this suggests a potential scaling trend where the improvement of **ITL** over random batch selection grows as models are fine-tuned on a larger pool of data.

Towards task-driven few-shot learning Being able to efficiently and automatically select data allows dynamic few-shot fine-tuning to individual tasks (Vinyals et al., 2016; Hardt & Sun, 2024), e.g., fine-tuning the model to each test point / query / prompt. Such task-driven few-shot learning can be seen as a form of “memory recall” akin to associative memory (Hopfield, 1982). Our results are

a first indication that task-driven learning can lead to substantial performance gains, and we believe that this is a promising direction for future studies.

5 RELATED WORK

Data retrieval Substantial prior work has studied data retrieval, e.g., in vector databases, using approximate nearest neighbor search (Johnson et al., 2019; Guo et al., 2020; Aumüller et al., 2020) where cosine similarity is a standard metric. Following the link between cosine similarity and **CTL**, **ITL** can be seen as a generalization of cosine similarity-based retrieval to batch and query sizes larger than one. Few-shot fine-tuning can be implemented also for sequences of *different* tasks (Vinyals et al., 2016), and as such task-driven few-shot fine-tuning can be seen as a form of “memory recall” akin to associative memory (Hopfield, 1982).

Undirected active learning Our work extends several previous works in active learning and experimental design (Chaloner & Verdinelli, 1995; Settles, 2009). Uncertainty sampling (US, Lewis & Catlett, 1994) is one of the most popular active learning methods. US selects points x with high *prior* uncertainty: $x_n = \arg \max_{x \in \mathcal{S}} \sigma_{n-1}^2(x)$. This is in stark contrast to **ITL** which selects points x that minimize *posterior* uncertainty about \mathcal{A} . It can be seen that US is the special “undirected” (i.e., $\mathcal{S} \subseteq \mathcal{A}$) case of **ITL** when the observation noise is homoscedastic (cf. Appendix D.2).

Several works have previously found entropy-based decision rules to be useful for undirected active learning (Krause & Guestrin, 2007; Guo & Greiner, 2007; Krause et al., 2008) and semi-supervised learning (Grandvalet & Bengio, 2004). A variance-based variant of **ITL** has previously been proposed by Yu et al. (2006) in the special case of global active learning without proving theoretical guarantees. Shoham & Avron (2023) recently analyzed experimental designs for global one-shot learning in overparameterized models.

Substantial work on active learning has studied entropy-based criteria in *parameter-space*, most notably BALD (Houlsby et al., 2011; Kirsch et al., 2019), which selects actions $x_n = \arg \max_{x \in \mathcal{X}} \mathbb{I}(\theta; y_x | \mathcal{D}_{n-1})$, where θ is the random parameter vector of a parametric model (e.g., via Bayesian deep learning). Such methods are inherently “undirected” in the sense that they do not facilitate learning on specific prediction targets. In contrast, **ITL** operates in *output-space* where it is straightforward to specify prediction targets, and which is computationally easier.

Transductive active learning In contrast, **ITL** operates in *output-space* where it is straightforward to specify prediction targets, and which is computationally easier. Special cases of **ITL** when $\mathcal{S} = \mathcal{X}$ and $|\mathcal{A}| = 1$ have been proposed in the foundational work of MacKay (1992) on “directed” output-space active learning, and later studied empirically by Wang et al. (2021) and Smith et al. (2023). Kothawade et al. (2021) recently evaluated **ITL** empirically on realistic image classification tasks in a pre-training context.

Other work on directed active learning Special cases of **ITL** when $\mathcal{S} = \mathcal{X}$ and $|\mathcal{A}| = 1$ have been proposed in the foundational work of MacKay (1992) on “directed” output-space active learning, and later studied empirically by Wang et al. (2021) and Smith et al. (2023). Recently, “directed” active learning methods have been proposed for the problem of determining the optimum of an unknown function, also known as best-arm identification (Audibert et al., 2010) or pure exploration bandits (Bubeck et al., 2009). Entropy search methods (Hennig & Schuler, 2012; Hernández-Lobato et al., 2014) are widely used and select $x_n = \arg \max_{x \in \mathcal{X}} \mathbb{I}(x^*; y_x | \mathcal{D}_{n-1})$ in *input-space* where $x^* = \arg \max_x f_x$. Similarly to **ITL**, *output-space* entropy search methods (Hoffman & Ghahramani, 2015; Wang & Jegelka, 2017), which select $x_n = \arg \max_{x \in \mathcal{X}} \mathbb{I}(f^*; y_x | \mathcal{D}_{n-1})$ with $f^* = \max_x f_x$, are more computationally tractable. In fact, output-space entropy search is a special case of **ITL** with a stochastic target space (Hübner et al., 2024). When subsampling target spaces via Thompson sampling (Thompson, 1933; Russo et al., 2018), **ITL** approximates these output-space methods. Bogunovic et al. (2016) analyze TRUVAR in the context of Bayesian optimization and level set estimation. TRUVAR is akin to a variance-based variant of **ITL** with a similar notion of “target space”, but their algorithm and analysis rely on a threshold scheme which requires that $\mathcal{A} \subseteq \mathcal{S}$. Fiez et al. (2019) introduce the *transductive linear bandit* problem, which is a special case of transductive active learning limited to a linear function class and with the objective of determining the maximum within an initial candidate set. We mention additional more loosely related works in Appendix A.

6 LIMITATIONS

Better models In this work, we focus solely on sequential decision-making *given* some model, rather than asking how one should construct such a model so that it is representative of the ground truth. Learning stochastic models and approximations thereof have been the subject of much recent work (Blundell et al., 2015; Maddox et al., 2019; Daxberger et al., 2021; Antorán et al., 2022; Lin et al., 2023). Specifically, **ITL** benefits if the model f captures the right “correlations” between points and if its “uncertainty” about the prediction at a specific point is accurate.⁹

Efficient computation of **ITL with large \mathcal{A}** Naïve computation of the **ITL** decision rule for m points within \mathcal{S} takes $O(|\mathcal{A}|^3 + m)$ time and $O(|\mathcal{A}|^2)$ space (cf. Appendix G) which is prohibitive for large $|\mathcal{A}|$. A practical solution for large \mathcal{A} is to subsample \mathcal{A} (such as in Section 4) within each round, and we provide a formal analysis of this approach for large \mathcal{A} in Appendix F.¹⁰

7 CONCLUSION AND FUTURE WORK

We framed the active fine-tuning problem as a generalization of active learning, *transductive active learning*, and proposed **ITL**, an approach which samples adaptively to maximize information gained about specified downstream tasks. We proved novel generalization bounds which may be of independent interest for active learning. Finally, we showed that **ITL** synthesizes prior works on *diversity-oriented* active learning and *relevance-oriented* retrieval, and demonstrated empirically that **ITL** substantially improves the efficiency of fine-tuning neural networks.

We believe that the transductive active learning methodology can also improve data-efficiency *beyond supervised learning*, such as in semi-supervised or self-supervised learning and reinforcement learning from human feedback (Dwaracherla et al., 2024), and leave this as an exciting direction for future work. The synthesis of retrieval and learning methods suggests applicability *beyond fine-tuning* such as for in-context learning (Brown et al., 2020) and retrieval-augmented generation (Lewis et al., 2020) as well as pre-training.

ACKNOWLEDGEMENTS

Many thanks to Armin Lederer, Johannes Kirschner, Jonas Rothfuss, Lars Lorch, Manish Prajapat, Nicolas Emmenegger, Parnian Kassraie, and Scott Sussex for their insightful feedback on different versions of this manuscript, as well as Anton Baumann for helpful discussions.

This project was supported in part by the European Research Council (ERC) under the European Union’s Horizon 2020 research and Innovation Program Grant agreement no. 815943, the Swiss National Science Foundation under NCCR Automation, grant agreement 51NF40 180545, and by a grant of the Hasler foundation (grant no. 21039). Jonas Hübötter was supported in part by the German Academic Scholarship Foundation (Studienstiftung).

REFERENCES

- Yasin Abbasi-Yadkori. *Online learning for linearly parametrized control problems*. PhD thesis, University of Alberta, 2013.
- Javier Antorán, David Janz, James U Allingham, Erik Daxberger, Riccardo Rb Barbano, Eric Nalisnick, and José Miguel Hernández-Lobato. Adapting the linearised laplace model evidence for modern deep learning. In *ICML*, 2022.
- Sanjeev Arora, Simon S Du, Wei Hu, Zhiyuan Li, Russ R Salakhutdinov, and Ruosong Wang. On exact computation with an infinitely wide neural net. *NeurIPS*, 32, 2019.
- David Arthur, Sergei Vassilvitskii, et al. k-means++: The advantages of careful seeding. In *SODA*, volume 7, 2007.

⁹For example, the results from Section 4 rely on embeddings being trained to capture the distribution shift.

¹⁰In our NN experiments, we subsample \mathcal{A} to a small set with size equal to the number of classes.

- Jordan T Ash, Chicheng Zhang, Akshay Krishnamurthy, John Langford, and Alekh Agarwal. Deep batch active learning by diverse, uncertain gradient lower bounds. *ICLR*, 2020.
- Jean-Yves Audibert, Sébastien Bubeck, and Rémi Munos. Best arm identification in multi-armed bandits. In *COLT*, 2010.
- Martin Aumüller, Erik Bernhardsson, and Alexander Faithfull. Ann-benchmarks: A benchmarking tool for approximate nearest neighbor algorithms. *Information Systems*, 87, 2020.
- Randall Balestriero, Mark Ibrahim, Vlad Sobal, Ari Morcos, Shashank Shekhar, Tom Goldstein, Florian Bordes, Adrien Bardes, Gregoire Mialon, Yuandong Tian, et al. A cookbook of self-supervised learning. *arXiv preprint arXiv:2304.12210*, 2023.
- Yoshua Bengio, Jérôme Louradour, Ronan Collobert, and Jason Weston. Curriculum learning. In *ICML*, volume 26, 2009.
- Mario Beraha, Alberto Maria Metelli, Matteo Papini, Andrea Tirinzoni, and Marcello Restelli. Feature selection via mutual information: New theoretical insights. In *IJCNN*, 2019.
- Charles Blundell, Julien Cornebise, Koray Kavukcuoglu, and Daan Wierstra. Weight uncertainty in neural network. In *ICML*, 2015.
- Ilija Bogunovic, Jonathan Scarlett, Andreas Krause, and Volkan Cevher. Truncated variance reduction: A unified approach to bayesian optimization and level-set estimation. *NeurIPS*, 29, 2016.
- Tom Brown, Benjamin Mann, Nick Ryder, Melanie Subbiah, Jared D Kaplan, Prafulla Dhariwal, Arvind Neelakantan, Pranav Shyam, Girish Sastry, Amanda Askell, et al. Language models are few-shot learners. *NeurIPS*, 33, 2020.
- Sébastien Bubeck, Rémi Munos, and Gilles Stoltz. Pure exploration in multi-armed bandits problems. In *ALT*, volume 20, 2009.
- Kathryn Chaloner and Isabella Verdinelli. Bayesian experimental design: A review. *Statistical Science*, 1995.
- Yuxin Chen and Andreas Krause. Near-optimal batch mode active learning and adaptive submodular optimization. In *ICML*, 2013.
- Sayak Ray Chowdhury and Aditya Gopalan. On kernelized multi-armed bandits. In *ICML*, 2017.
- Cody Coleman, Edward Chou, Julian Katz-Samuels, Sean Culatana, Peter Bailis, Alexander C Berg, Robert Nowak, Roshan Sumbaly, Matei Zaharia, and I Zeki Yalniz. Similarity search for efficient active learning and search of rare concepts. In *AAAI*, volume 36, 2022.
- Thomas M Cover. *Elements of information theory*. John Wiley & Sons, 1999.
- Abhimanyu Das and David Kempe. Approximate submodularity and its applications: Subset selection, sparse approximation and dictionary selection. *JMLR*, 19(1), 2018.
- Erik Daxberger, Agustinus Kristiadi, Alexander Immer, Runa Eschenhagen, Matthias Bauer, and Philipp Hennig. Laplace redux-effortless bayesian deep learning. *NeurIPS*, 34, 2021.
- Jia Deng, Wei Dong, Richard Socher, Li-Jia Li, Kai Li, and Li Fei-Fei. Imagenet: A large-scale hierarchical image database. In *CVPR*, 2009.
- Jacob Devlin, Ming-Wei Chang, Kenton Lee, and Kristina Toutanova. BERT: Pre-training of deep bidirectional transformers for language understanding. In *NAACL*, 2019.
- Vikranth Dwaracherla, Seyed Mohammad Asghari, Botao Hao, and Benjamin Van Roy. Efficient exploration for llms. *arXiv preprint arXiv:2402.00396*, 2024.
- Nicolas Emmenegger, Mojmír Mutný, and Andreas Krause. Likelihood ratio confidence sets for sequential decision making. *NeurIPS*, 37, 2023.

- Hossein Esfandiari, Amin Karbasi, and Vahab Mirrokni. Adaptivity in adaptive submodularity. In *COLT*, 2021.
- Tanner Fiez, Lalit Jain, Kevin G Jamieson, and Lillian Ratliff. Sequential experimental design for transductive linear bandits. *NeurIPS*, 32, 2019.
- Mingfei Gao, Zizhao Zhang, Guo Yu, Sercan Ö Arık, Larry S Davis, and Tomas Pfister. Consistency-based semi-supervised active learning: Towards minimizing labeling cost. In *ECCV*, 2020.
- Yonatan Geifman and Ran El-Yaniv. Deep active learning over the long tail. *arXiv preprint arXiv:1711.00941*, 2017.
- Daniel Golovin and Andreas Krause. Adaptive submodularity: Theory and applications in active learning and stochastic optimization. *JAIR*, 42, 2011.
- Yves Grandvalet and Yoshua Bengio. Semi-supervised learning by entropy minimization. *NeurIPS*, 17, 2004.
- Alex Graves, Marc G Bellemare, Jacob Menick, Remi Munos, and Koray Kavukcuoglu. Automated curriculum learning for neural networks. In *ICML*, 2017.
- Franklin A Graybill. *An introduction to linear statistical models*. Literary Licensing, LLC, 1961.
- Ruiqi Guo, Philip Sun, Erik Lindgren, Quan Geng, David Simcha, Felix Chern, and Sanjiv Kumar. Accelerating large-scale inference with anisotropic vector quantization. In *ICML*, 2020.
- Yuhong Guo and Russell Greiner. Optimistic active-learning using mutual information. In *IJCAI*, volume 7, 2007.
- Moritz Hardt and Yu Sun. Test-time training on nearest neighbors for large language models. *ICLR*, 2024.
- Bobby He, Balaji Lakshminarayanan, and Yee Whye Teh. Bayesian deep ensembles via the neural tangent kernel. *NeurIPS*, 33, 2020.
- Dan Hendrycks and Thomas Dietterich. Benchmarking neural network robustness to common corruptions and perturbations. *ICLR*, 2019.
- Dan Hendrycks and Kevin Gimpel. A baseline for detecting misclassified and out-of-distribution examples in neural networks. *ICLR*, 2017.
- Philipp Hennig and Christian J Schuler. Entropy search for information-efficient global optimization. *JMLR*, 13(6), 2012.
- José Miguel Hernández-Lobato, Matthew W Hoffman, and Zoubin Ghahramani. Predictive entropy search for efficient global optimization of black-box functions. *NeurIPS*, 27, 2014.
- Matthew W Hoffman and Zoubin Ghahramani. Output-space predictive entropy search for flexible global optimization. In *NeurIPS workshop on Bayesian Optimization*, 2015.
- David Holzmüller, Viktor Zaverkin, Johannes Kästner, and Ingo Steinwart. A framework and benchmark for deep batch active learning for regression. *JMLR*, 24(164), 2023.
- John J Hopfield. Neural networks and physical systems with emergent collective computational abilities. *Proceedings of the national academy of sciences*, 79(8), 1982.
- Neil Houlsby, Ferenc Huszár, Zoubin Ghahramani, and Máté Lengyel. Bayesian active learning for classification and preference learning. *CoRR*, 2011.
- Jeremy Howard and Sebastian Ruder. Universal language model fine-tuning for text classification. In *ACL*, 2018.
- Jonas Hübner, Bhavya Sukhija, Lenart Treven, Yarden As, and Andreas Krause. Transductive active learning: Theory and applications. *arXiv preprint arXiv:2402.15898*, 2024.

- Arthur Jacot, Franck Gabriel, and Clément Hongler. Neural tangent kernel: Convergence and generalization in neural networks. *NeurIPS*, 31, 2018.
- Jeff Johnson, Matthijs Douze, and Hervé Jégou. Billion-scale similarity search with gpus. *IEEE Transactions on Big Data*, 7(3), 2019.
- Jean Kaddour, Steindór Sæmundsson, et al. Probabilistic active meta-learning. *NeurIPS*, 33, 2020.
- Parnian Kassraie and Andreas Krause. Neural contextual bandits without regret. In *AISTATS*, 2022.
- Mohammad Emtiyaz E Khan, Alexander Immer, Ehsan Abedi, and Maciej Korzepa. Approximate inference turns deep networks into gaussian processes. *NeurIPS*, 32, 2019.
- Rajiv Khanna, Ethan Elenberg, Alex Dimakis, Sahand Negahban, and Joydeep Ghosh. Scalable greedy feature selection via weak submodularity. In *AISTATS*, 2017.
- Diederik P Kingma and Jimmy Ba. Adam: A method for stochastic optimization. In *ICLR*, 2014.
- Andreas Kirsch, Joost Van Amersfoort, and Yarin Gal. Batchbald: Efficient and diverse batch acquisition for deep bayesian active learning. *NeurIPS*, 32, 2019.
- Pang Wei Koh, Shiori Sagawa, Henrik Marklund, Sang Michael Xie, Marvin Zhang, Akshay Bal-subramani, Weihua Hu, Michihiro Yasunaga, Richard Lanus Phillips, Irena Gao, et al. Wilds: A benchmark of in-the-wild distribution shifts. In *ICML*, 2021.
- Simon Kornblith, Jonathon Shlens, and Quoc V Le. Do better imagenet models transfer better? In *CVPR*, 2019.
- Suraj Kothawade, Nathan Beck, Krishnateja Killamsetty, and Rishabh Iyer. Similar: Submodular information measures based active learning in realistic scenarios. *NeurIPS*, 34, 2021.
- Andreas Krause and Daniel Golovin. Submodular function maximization. *Tractability*, 3, 2014.
- Andreas Krause and Carlos Guestrin. Nonmyopic active learning of gaussian processes: an exploration-exploitation approach. In *ICML*, volume 24, 2007.
- Andreas Krause, Ajit Singh, and Carlos Guestrin. Near-optimal sensor placements in gaussian processes: Theory, efficient algorithms and empirical studies. *JMLR*, 9(2), 2008.
- Alex Krizhevsky, Geoffrey Hinton, et al. Learning multiple layers of features from tiny images. Technical report, University of Toronto, 2009.
- Yann LeCun, Corinna Cortes, and Christopher J.C. Burges. The mnist database of handwritten digits. <http://yann.lecun.com/exdb/mnist/>, 1998.
- Jaehoon Lee, Yasaman Bahri, Roman Novak, Samuel S Schoenholz, Jeffrey Pennington, and Jascha Sohl-Dickstein. Deep neural networks as gaussian processes. *ICLR*, 2018.
- Jaehoon Lee, Lechao Xiao, Samuel Schoenholz, Yasaman Bahri, Roman Novak, Jascha Sohl-Dickstein, and Jeffrey Pennington. Wide neural networks of any depth evolve as linear models under gradient descent. *NeurIPS*, 32, 2019.
- Yoonho Lee, Annie S Chen, Fahim Tajwar, Ananya Kumar, Huaxiu Yao, Percy Liang, and Chelsea Finn. Surgical fine-tuning improves adaptation to distribution shifts. *NeurIPS workshop on Distribution Shifts*, 2022.
- D Lewis and W Gale. A sequential algorithm for training text classifiers. In *SIGIR*, 1994.
- David D Lewis and Jason Catlett. Heterogeneous uncertainty sampling for supervised learning. In *Machine learning proceedings*. 1994.
- Patrick Lewis, Ethan Perez, Aleksandra Piktus, Fabio Petroni, Vladimir Karpukhin, Naman Goyal, Heinrich Küttler, Mike Lewis, Wen-tau Yih, Tim Rocktäschel, et al. Retrieval-augmented generation for knowledge-intensive nlp tasks. *NeurIPS*, 33, 2020.

- Jihao Andreas Lin, Javier Antorán, Shreyas Padhy, David Janz, José Miguel Hernández-Lobato, and Alexander Terenin. Sampling from gaussian process posteriors using stochastic gradient descent. *NeurIPS*, 37, 2023.
- David JC MacKay. Information-based objective functions for active data selection. *Neural computation*, 4(4), 1992.
- Wesley J Maddox, Pavel Izmailov, Timur Garipov, Dmitry P Vetrov, and Andrew Gordon Wilson. A simple baseline for bayesian uncertainty in deep learning. *NeurIPS*, 32, 2019.
- Sadhika Malladi, Alexander Wettig, Dingli Yu, Danqi Chen, and Sanjeev Arora. A kernel-based view of language model fine-tuning. In *ICML*, 2023.
- James Martens and Roger Grosse. Optimizing neural networks with kronecker-factored approximate curvature. In *ICML*, 2015.
- Mojmir Mutny and Andreas Krause. Experimental design for linear functionals in reproducing kernel hilbert spaces. *NeurIPS*, 35, 2022.
- George L Nemhauser, Laurence A Wolsey, and Marshall L Fisher. An analysis of approximations for maximizing submodular set functions—i. *Mathematical programming*, 14, 1978.
- Rafail Ostrovsky, Yuval Rabani, Leonard J Schulman, and Chaitanya Swamy. The effectiveness of lloyd-type methods for the k-means problem. *JACM*, 2013.
- Aldo Pacchiano, Jonathan N Lee, and Emma Brunskill. Experiment planning with function approximation. *NeurIPS*, 37, 2024.
- Hanchuan Peng, Fuhui Long, and Chris Ding. Feature selection based on mutual information criteria of max-dependency, max-relevance, and min-redundancy. *IEEE Transactions on pattern analysis and machine intelligence*, 27(8), 2005.
- Ali Rahimi and Benjamin Recht. Random features for large-scale kernel machines. *NeurIPS*, 20, 2007.
- Benjamin Recht, Rebecca Roelofs, Ludwig Schmidt, and Vaishal Shankar. Do imagenet classifiers generalize to imagenet? In *ICML*, 2019.
- Jonas Rothfuss, Christopher Koenig, Alisa Rupenyan, and Andreas Krause. Meta-learning priors for safe bayesian optimization. In *COLT*, 2023.
- Daniel J Russo, Benjamin Van Roy, Abbas Kazerouni, Ian Osband, Zheng Wen, et al. A tutorial on thompson sampling. *Foundations and Trends® in Machine Learning*, 11(1), 2018.
- Tobias Scheffer, Christian Decomain, and Stefan Wrobel. Active hidden markov models for information extraction. In *IDA*, 2001.
- Ozan Sener and Silvio Savarese. Active learning for convolutional neural networks: A core-set approach. *ICLR*, 2017.
- Burr Settles. Active learning literature survey. Technical report, University of Wisconsin-Madison Department of Computer Sciences, 2009.
- Burr Settles and Mark Craven. An analysis of active learning strategies for sequence labeling tasks. In *EMNLP*, 2008.
- Zhiqiang Shen, Zechun Liu, Jie Qin, Marios Savvides, and Kwang-Ting Cheng. Partial is better than all: revisiting fine-tuning strategy for few-shot learning. In *AAAI*, volume 35, 2021.
- Neta Shoham and Haim Avron. Experimental design for overparameterized learning with application to single shot deep active learning. *IEEE Transactions on Pattern Analysis and Machine Intelligence*, 2023.
- Ravid Shwartz-Ziv and Yann LeCun. To compress or not to compress—self-supervised learning and information theory: A review. *arXiv preprint arXiv:2304.09355*, 2023.

- Julio Silva-Rodríguez, Jose Dolz, and Ismail Ben Ayed. Towards foundation models and few-shot parameter-efficient fine-tuning for volumetric organ segmentation. In *MICCAI*, 2023.
- Freddie Bickford Smith, Andreas Kirsch, Sebastian Farquhar, Yarin Gal, Adam Foster, and Tom Rainforth. Prediction-oriented bayesian active learning. In *AISTATS*, 2023.
- Petru Soviany, Radu Tudor Ionescu, Paolo Rota, and Nicu Sebe. Curriculum learning: A survey. *IJCV*, 2022.
- Niranjan Srinivas, Andreas Krause, Sham M Kakade, and Matthias Seeger. Gaussian process optimization in the bandit setting: No regret and experimental design. In *ICML*, volume 27, 2009.
- Alex Tamkin, Dat Nguyen, Salil Deshpande, Jesse Mu, and Noah Goodman. Active learning helps pretrained models learn the intended task. *NeurIPS*, 35, 2022.
- Mingxing Tan and Quoc Le. Efficientnet: Rethinking model scaling for convolutional neural networks. In *ICML*, 2019.
- William R Thompson. On the likelihood that one unknown probability exceeds another in view of the evidence of two samples. *Biometrika*, 1933.
- Sattar Vakili, Kia Khezeli, and Victor Picheny. On information gain and regret bounds in gaussian process bandits. In *AISTATS*, 2021.
- Vladimir Vapnik. *Estimation of dependences based on empirical data*. Springer Science & Business Media, 1982.
- Jorge R Vergara and Pablo A Estévez. A review of feature selection methods based on mutual information. *Neural computing and applications*, 24, 2014.
- Oriol Vinyals, Charles Blundell, Timothy Lillicrap, Daan Wierstra, et al. Matching networks for one shot learning. *NeurIPS*, 29, 2016.
- Martin J Wainwright. *High-dimensional statistics: A non-asymptotic viewpoint*, volume 48. Cambridge university press, 2019.
- Chaoqi Wang, Shengyang Sun, and Roger Grosse. Beyond marginal uncertainty: How accurately can bayesian regression models estimate posterior predictive correlations? In *AISTATS*, 2021.
- Zi Wang and Stefanie Jegelka. Max-value entropy search for efficient bayesian optimization. In *ICML*, 2017.
- Alexander Wei, Wei Hu, and Jacob Steinhardt. More than a toy: Random matrix models predict how real-world neural representations generalize. In *ICML*, 2022.
- Christopher KI Williams and Carl Edward Rasmussen. *Gaussian processes for machine learning*, volume 2. MIT press Cambridge, MA, 2006.
- Hwanjo Yu and Sungchul Kim. Passive sampling for regression. In *ICDM*, 2010.
- Kai Yu, Jinbo Bi, and Volker Tresp. Active learning via transductive experimental design. In *ICML*, volume 23, 2006.
- Andrea Zanette, Kefan Dong, Jonathan N Lee, and Emma Brunskill. Design of experiments for stochastic contextual linear bandits. *NeurIPS*, 34, 2021.
- Haizhong Zheng, Rui Liu, Fan Lai, and Atul Prakash. Coverage-centric coresnet selection for high pruning rates. *ICLR*, 2023.

APPENDICES

A general principle of “transductive learning” was already formulated by the famous computer scientist Vladimir Vapnik in the 20th century. Vapnik proposes the following “imperative for a complex world”:

When solving a problem of interest, do not solve a more general problem as an intermediate step. Try to get the answer that you really need but not a more general one.

– Vapnik (1982)

These appendices provide additional background, proofs, experiment details, and ablation studies.

CONTENTS

A Additional Related Work	15
B Background	15
B.1 Information Theory	15
B.2 Gaussian Processes	15
C Provably Efficient Non-adaptive Batch Selection and its Relation to Submodularity	16
D Proofs	16
D.1 Definitions	16
D.2 Undirected Case of ITL	17
D.3 Proof of Theorem 3.1	17
D.4 Proof of Theorem 3.2	21
D.5 Useful Facts and Inequalities	22
E Correlation-based Transductive Learning	23
F Subsampling Target Spaces	23
F.1 Stochastic Target Spaces	23
G Computational Complexity	24
H Additional NN Experiments & Details	24
H.1 Experiment Details	24
H.2 Embeddings and Kernels	26
H.3 Towards Uncertainty Quantification in Latent Space	27
H.4 Batch Selection via Conditional Embeddings	28
H.5 Baselines	28
H.6 Additional experiments	30
H.7 Ablation study of noise standard deviation ρ	31

A ADDITIONAL RELATED WORK

The general principle of non-active “transductive learning” was introduced by Vapnik (1982). The notion of “target” from transductive active learning is akin to the notion of “task” in curriculum learning (Bengio et al., 2009; Graves et al., 2017; Soviany et al., 2022). The study of settings where the irreducible uncertainty is zero is related to the study of estimability in experimental design (Graybill, 1961; Mutny & Krause, 2022). In feature selection, selecting features that maximize information gain with respect to a to-be-predicted label is a standard approach (Peng et al., 2005; Vergara & Estévez, 2014; Beraha et al., 2019) which is akin to **ITL**. Balancing relevance and informativeness, similarly to **ITL**, is also important for data pruning (Zheng et al., 2023). Transductive active learning is complementary to other learning methodologies, such as semi-supervised learning (Gao et al., 2020), self-supervised learning (Shwartz-Ziv & LeCun, 2023; Balestrieri et al., 2023), and meta-learning (Kaddour et al., 2020; Rothfuss et al., 2023).

B BACKGROUND

B.1 INFORMATION THEORY

Throughout this work, \log denotes the natural logarithm. Given random vectors \mathbf{x} and \mathbf{y} , we denote by

$$\begin{aligned} H[\mathbf{x}] &\stackrel{\text{def}}{=} \mathbb{E}_{p(\mathbf{x})}[-\log p(\mathbf{x})], \\ H[\mathbf{x} \mid \mathbf{y}] &\stackrel{\text{def}}{=} \mathbb{E}_{p(\mathbf{x}, \mathbf{y})}[-\log p(\mathbf{x} \mid \mathbf{y})], \quad \text{and} \\ I(\mathbf{x}; \mathbf{y}) &\stackrel{\text{def}}{=} H[\mathbf{x}] - H[\mathbf{x} \mid \mathbf{y}] \end{aligned}$$

the (differential) entropy, conditional entropy, and information gain, respectively (Cover, 1999).¹¹

B.2 GAUSSIAN PROCESSES

The stochastic process f is a Gaussian process (GP, Williams & Rasmussen (2006)), denoted $f \sim \mathcal{GP}(\mu, k)$, with mean function μ and kernel k if for any finite subset $X = \{\mathbf{x}_1, \dots, \mathbf{x}_n\} \subseteq \mathcal{X}$, $\mathbf{f}_X \sim \mathcal{N}(\mu_X, \mathbf{K}_{XX})$ is jointly Gaussian with mean vector $\mu_X(i) = \mu(\mathbf{x}_i)$ and covariance matrix $\mathbf{K}_{XX}(i, j) = k(\mathbf{x}_i, \mathbf{x}_j)$.

In the following, we formalize the assumptions from the GP setting (cf. Section 3.1).

Assumption B.1 (Gaussian prior). We assume that $f \sim \mathcal{GP}(\mu, k)$ with known mean function μ and kernel k .

Assumption B.2 (Gaussian noise). We assume that the noise $\varepsilon_{\mathbf{x}}$ is mutually independent and zero-mean Gaussian with known variance $\rho^2(\mathbf{x}) > 0$. We write $\mathbf{P}_X = \text{diag}\{\rho^2(\mathbf{x}_1), \dots, \rho^2(\mathbf{x}_n)\}$.

Under Assumptions B.1 and B.2, the posterior distribution of f after observing points X is $\mathcal{GP}(\mu_n, k_n)$ with

$$\begin{aligned} \mu_n(\mathbf{x}) &= \mu(\mathbf{x}) + \mathbf{K}_{\mathbf{x}X}(\mathbf{K}_{XX} + \mathbf{P}_X)^{-1}(\mathbf{y}_X - \mu_X), \\ k_n(\mathbf{x}, \mathbf{x}') &= k(\mathbf{x}, \mathbf{x}') - \mathbf{K}_{\mathbf{x}X}(\mathbf{K}_{XX} + \mathbf{P}_X)^{-1}\mathbf{K}_{X\mathbf{x}'}, \\ \sigma_n^2(\mathbf{x}) &= k_n(\mathbf{x}, \mathbf{x}). \end{aligned}$$

For Gaussian random vectors \mathbf{f} and \mathbf{y} , the entropy is $H[\mathbf{f}] = \frac{n}{2} \log(2\pi e) + \frac{1}{2} \log |\text{Var}[\mathbf{f}]|$, the information gain is $I(\mathbf{f}; \mathbf{y}) = \frac{1}{2}(\log |\text{Var}[\mathbf{y}]| - \log |\text{Var}[\mathbf{y} \mid \mathbf{f}]|)$, and

$$\gamma_n = \max_{\substack{X \subseteq \mathcal{X} \\ |X| \leq n}} \frac{1}{2} \log |\mathbf{I} + \mathbf{P}_X^{-1} \mathbf{K}_{XX}|.$$

¹¹One has to be careful to ensure that $I(\mathbf{x}; \mathbf{y})$ exists, i.e., $|I(\mathbf{x}; \mathbf{y})| < \infty$. We will assume that this is the case throughout this work. When \mathbf{x} and \mathbf{y} are jointly Gaussian, this is satisfied when the noise variance ρ^2 is positive.

C PROVABLY EFFICIENT NON-ADAPTIVE BATCH SELECTION AND ITS RELATION TO SUBMODULARITY

Recall the non-adaptive optimization problem

$$B_{n,k} = \arg \max_{\substack{B \subseteq \mathcal{S} \\ |B|=k}} I(\mathbf{f}_A; \mathbf{y}_B \mid \mathcal{D}_{n-1})$$

from Equation (3), and denote by $B'_{n,k} = \mathbf{x}_{n,1:k}$ the greedy approximation from Equation (4). Note that the objective function

$$F_n(B) \stackrel{\text{def}}{=} I(\mathbf{f}_A; \mathbf{y}_B \mid \mathcal{D}_{n-1}) = H[\mathbf{f}_A \mid \mathcal{D}_{n-1}] - H[\mathbf{f}_A \mid \mathcal{D}_{n-1}, \mathbf{y}_B]$$

is non-negative and monotone,¹² since conditional entropy is monotone (which is also called the “information never hurts” principle).

Let $\Delta_n(\mathbf{x} \mid B) \stackrel{\text{def}}{=} \Delta_n(\{\mathbf{x}\} \mid B) \stackrel{\text{def}}{=} F_n(B \cup \{\mathbf{x}\}) - F_n(B)$ denote the *marginal gain* of $\mathbf{x} \in \mathcal{S}$ given $B \subseteq \mathcal{S}$ which simplifies to

$$\begin{aligned} \Delta_n(\mathbf{x} \mid B) &= I(\mathbf{f}_A; \mathbf{y}_B, \mathbf{y}_x \mid \mathcal{D}_{n-1}) - I(\mathbf{f}_A; \mathbf{y}_B \mid \mathcal{D}_{n-1}) \\ &= H[\mathbf{f}_A \mid \mathcal{D}_{n-1}, \mathbf{y}_B] - H[\mathbf{f}_A \mid \mathcal{D}_{n-1}, \mathbf{y}_B, \mathbf{y}_x] \\ &= I(\mathbf{f}_A; \mathbf{y}_x \mid \mathcal{D}_{n-1}, \mathbf{y}_B) \end{aligned}$$

and which is precisely the objective function of **ITL** from Equation (4).

Batch selection via conditional embeddings approximates $B_{n,k}$ Building upon the theory of maximizing monotone submodular functions (Nemhauser et al., 1978; Krause & Golovin, 2014), Das & Kempe (2018) study greedy maximization under “approximate” submodularity:

Definition C.1 (Submodularity ratio of **ITL**). Das & Kempe (2018) define the *submodularity ratio* of F_n up to cardinality $k \geq 1$ as

$$\kappa_n(k) \stackrel{\text{def}}{=} \min_{\substack{B \subseteq B'_{n,k} \\ X \subseteq \mathcal{S}: |X| \leq k \\ B \cap X = \emptyset}} \frac{\sum_{\mathbf{x} \in X} \Delta_n(\mathbf{x} \mid B)}{\Delta_n(X \mid B)}, \quad (5)$$

where they define $\frac{0}{0} \equiv 1$.

As a special case of theorem 6 from Das & Kempe (2018), applying that F_n is non-negative and monotone, we obtain the following result.

Theorem C.2 (Efficiency of batch selection via conditional embeddings). *For any $n, k \geq 1$, the greedy solution $B'_{n,k}$ provides a $(1 - e^{-\kappa_n(k)})$ -approximation of $B_{n,k}$.*

If $\mathcal{S} \subseteq \mathcal{A}$, it is well known (e.g., Srinivas et al., 2009) that F_n is submodular, which implies that $\kappa_n(k) \geq 1$ for all $k \geq 1$.

D PROOFS

D.1 DEFINITIONS

We write

- $\sigma^2 \stackrel{\text{def}}{=} \max_{\mathbf{x} \in \mathcal{X}} \sigma_0^2(\mathbf{x})$, and
- $\tilde{\sigma}^2 \stackrel{\text{def}}{=} \max_{\mathbf{x} \in \mathcal{X}} \sigma_0^2(\mathbf{x}) + \rho^2(\mathbf{x})$.

¹²Formally, $F_n(B) \geq 0$ and $F_n(B') \leq F_n(B)$ for any $B' \subseteq B \subseteq \mathcal{S}$.

D.2 UNDIRECTED CASE OF **ITL**

We briefly examine the important special case of **ITL** where $\mathcal{S} \subseteq \mathcal{A}$. In this setting, for all $\mathbf{x} \in \mathcal{S}$, the decision rule of **ITL** simplifies to

$$\begin{aligned} I(\mathbf{f}_{\mathcal{A}}; y_{\mathbf{x}} \mid \mathcal{D}_n) &\stackrel{(i)}{=} I(\mathbf{f}_{\mathcal{A} \setminus \{\mathbf{x}\}}; y_{\mathbf{x}} \mid \mathbf{f}_{\mathbf{x}}, \mathcal{D}_n) + I(\mathbf{f}_{\mathbf{x}}; y_{\mathbf{x}} \mid \mathcal{D}_n) \\ &\stackrel{(ii)}{=} I(\mathbf{f}_{\mathbf{x}}; y_{\mathbf{x}} \mid \mathcal{D}_n) \\ &= H[y_{\mathbf{x}} \mid \mathcal{D}_n] - H[\varepsilon_{\mathbf{x}}] \end{aligned}$$

where (i) follows from the chain rule of information gain and $\mathbf{x} \in \mathcal{S} \subseteq \mathcal{A}$; and (ii) follows from the conditional independence $\mathbf{f}_{\mathcal{A}} \perp y_{\mathbf{x}} \mid \mathbf{f}_{\mathbf{x}}$.

If additionally f is a GP then

$$H[y_{\mathbf{x}} \mid \mathcal{D}_n] - H[\varepsilon_{\mathbf{x}}] = \frac{1}{2} \log \left(1 + \frac{\text{Var}[\mathbf{f}_{\mathbf{x}} \mid \mathcal{D}_n]}{\text{Var}[\varepsilon_{\mathbf{x}}]} \right).$$

Therefore, when $\mathcal{S} \subseteq \mathcal{A}$ and observation noise is homoscedastic, **ITL** is equivalent to uncertainty sampling.

D.3 PROOF OF THEOREM 3.1

We will now prove Theorem 3.1 where we assume throughout that $\mathcal{S} \subseteq \mathcal{A}$. Let

$$\Gamma_n \stackrel{\text{def}}{=} \max_{\mathbf{x} \in \mathcal{S}} I(\mathbf{f}_{\mathcal{A}}; y_{\mathbf{x}} \mid \mathcal{D}_n) \quad (6)$$

denote the objective value of **ITL** during round $n + 1$.

Before proving the convergence outside \mathcal{S} in Appendix D.3.1, we first prove the convergence of the “step-wise uncertainty reduction” Γ_n .

Theorem D.1 (Bound of uncertainty reduction for **ITL**). *For any $n \geq 1$, if **ITL** generated the sequence $\{\mathbf{x}_i\}_{i=1}^n$ then*

$$\Gamma_{n-1} \leq \frac{\gamma_n}{n}. \quad (7)$$

Proof. We have

$$\begin{aligned} \Gamma_{n-1} &= \frac{1}{n} \sum_{i=0}^{n-1} \Gamma_{n-1} \\ &\stackrel{(i)}{\leq} \frac{1}{n} \sum_{i=0}^{n-1} \Gamma_i \\ &\stackrel{(ii)}{=} \frac{1}{n} \sum_{i=0}^{n-1} I(\mathbf{f}_{\mathcal{A}}; y_{\mathbf{x}_{i+1}} \mid \mathcal{D}_i) \\ &\stackrel{(iii)}{=} \frac{1}{n} \sum_{i=0}^{n-1} I(\mathbf{f}_{\mathcal{A}}; y_{\mathbf{x}_{i+1}} \mid \mathbf{y}_{\mathbf{x}_{1:i}}) \\ &\stackrel{(iv)}{=} \frac{1}{n} I(\mathbf{f}_{\mathcal{A}}; \mathbf{y}_{\mathbf{x}_{1:n}}) \\ &\leq \frac{1}{n} \max_{\substack{X \subseteq \mathcal{S} \\ |X|=n}} I(\mathbf{f}_{\mathcal{A}}; \mathbf{y}_X) \\ &\stackrel{(v)}{\leq} \frac{1}{n} \max_{\substack{X \subseteq \mathcal{S} \\ |X|=n}} I(\mathbf{f}_X; \mathbf{y}_X) \\ &= \frac{\gamma_n}{n} \end{aligned}$$

where (i) follows from the monotonicity of conditional information gain since $\mathcal{S} \subseteq \mathcal{A}$ which implies $\mathbf{y}_{x_{1:i}} \perp y_x \mid \mathbf{f}_{\mathcal{A}}$ for all $\mathbf{x} \in \mathcal{S}$; (ii) uses the objective of **ITL**; (iii) uses that the posterior variance of Gaussians is independent of the realization and only depends on the *location* of observations; (iv) uses the chain rule of information gain; (v) uses $\mathbf{y}_X \perp \mathbf{f}_{\mathcal{A}} \mid \mathbf{f}_X$ and the data processing inequality. The conditional independences follow from the assumption that the observation noise is independent. \square

We prove a simple consequence of Theorem D.1 for points \mathbf{x} that are *both* in the target space \mathcal{A} and in the sample space \mathcal{S} .

Lemma D.2 (Uniform bound of marginal variance within \mathcal{S}). *For any $n \geq 0$ and $\mathbf{x} \in \mathcal{A} \cap \mathcal{S}$,*

$$\sigma_n^2(\mathbf{x}) \leq 2\tilde{\sigma}^2 \cdot \Gamma_n. \quad (8)$$

Proof. We have

$$\begin{aligned} \sigma_n^2(\mathbf{x}) &= \text{Var}[f_{\mathbf{x}} \mid \mathcal{D}_n] - \underbrace{\text{Var}[f_{\mathbf{x}} \mid f_{\mathbf{x}}, \mathcal{D}_n]}_0 \\ &\stackrel{(i)}{=} \text{Var}[y_{\mathbf{x}} \mid \mathcal{D}_n] - \rho^2(\mathbf{x}) \\ &\quad - (\text{Var}[y_{\mathbf{x}} \mid f_{\mathbf{x}}, \mathcal{D}_n] - \rho^2(\mathbf{x})) \\ &= \text{Var}[y_{\mathbf{x}} \mid \mathcal{D}_n] - \text{Var}[y_{\mathbf{x}} \mid f_{\mathbf{x}}, \mathcal{D}_n] \\ &\stackrel{(ii)}{\leq} \tilde{\sigma}^2 \log \left(\frac{\text{Var}[y_{\mathbf{x}} \mid \mathcal{D}_n]}{\text{Var}[y_{\mathbf{x}} \mid f_{\mathbf{x}}, \mathcal{D}_n]} \right) \\ &= 2\tilde{\sigma}^2 \cdot \text{I}(f_{\mathbf{x}}; y_{\mathbf{x}} \mid \mathcal{D}_n) \\ &\stackrel{(iii)}{\leq} 2\tilde{\sigma}^2 \cdot \text{I}(\mathbf{f}_{\mathcal{A}}; y_{\mathbf{x}} \mid \mathcal{D}_n) \\ &\stackrel{(iv)}{\leq} 2\tilde{\sigma}^2 \cdot \max_{\mathbf{x}' \in \mathcal{S}} \text{I}(\mathbf{f}_{\mathcal{A}}; y_{\mathbf{x}'} \mid \mathcal{D}_n) \\ &= 2\tilde{\sigma}^2 \cdot \Gamma_n \end{aligned}$$

where (i) follows from the noise assumption (cf. Assumption B.2); (ii) follows from Lemma D.13 and using monotonicity of variance; (iii) follows from $\mathbf{x} \in \mathcal{A}$ and monotonicity of information gain; and (iv) follows from $\mathbf{x} \in \mathcal{S}$. \square

D.3.1 CONVERGENCE OUTSIDE \mathcal{S}

We will now show convergence of marginal variance to the irreducible uncertainty for points outside the sample space.

Our proof roughly proceeds as follows: We construct an “approximate Markov boundary” of \mathbf{x} in \mathcal{S} , and show (1) that the size of this Markov boundary is independent of n , and (2) that a small uncertainty reduction within the Markov boundary implies that the marginal variances at the Markov boundary and (!) \mathbf{x} are small.

Definition D.3 (Approximate Markov boundary). For any $\epsilon > 0$, $n \geq 0$, and $\mathbf{x} \in \mathcal{X}$, we denote by $B_{n,\epsilon}(\mathbf{x})$ the smallest (multi-)subset of \mathcal{S} such that

$$\text{Var}[f_{\mathbf{x}} \mid \mathcal{D}_n, \mathbf{y}_{B_{n,\epsilon}(\mathbf{x})}] \leq \eta_{\mathcal{S}}^2(\mathbf{x}) + \epsilon. \quad (9)$$

We call $B_{n,\epsilon}(\mathbf{x})$ an ϵ -approximate Markov boundary of \mathbf{x} in \mathcal{S} .

Equation (9) is akin to the notion of the smallest Markov blanket in \mathcal{S} of some $\mathbf{x} \in \mathcal{X}$ (called a *Markov boundary*) which is the smallest set $\mathcal{B} \subseteq \mathcal{S}$ such that $f_{\mathbf{x}} \perp \mathbf{f}_{\mathcal{S}} \mid \mathbf{f}_{\mathcal{B}}$.

Lemma D.4 (Existence of an approximate Markov boundary). *For any $\epsilon > 0$, let k be the smallest integer satisfying*

$$\frac{\gamma_k}{k} \leq \frac{\epsilon \lambda_{\min}^2(\text{Var}[\mathbf{f}_{\mathcal{S}}])}{2|\mathcal{S}|^2 \sigma^4 \tilde{\sigma}^2}. \quad (10)$$

Then, for any $n \geq 0$ and $\mathbf{x} \in \mathcal{X}$, there exists an ϵ -approximate Markov boundary $B_{n,\epsilon}(\mathbf{x})$ of \mathbf{x} in \mathcal{S} with size at most k .

Lemma D.4 shows that for any $\epsilon > 0$ there exists a universal constant b_ϵ such that

$$|B_{n,\epsilon}(\mathbf{x})| \leq b_\epsilon \quad \forall n \geq 0, \mathbf{x} \in \mathcal{X}. \quad (11)$$

We defer the proof of Lemma D.4 to Appendix D.3.3 where we also provide an algorithm to compute $B_{n,\epsilon}(\mathbf{x})$.

Lemma D.5. For any $\epsilon > 0$, $n \geq 0$, and $\mathbf{x} \in \mathcal{X}$,

$$\sigma_n^2(\mathbf{x}) \leq 2\sigma^2 \cdot \mathbf{I}(f_{\mathbf{x}}; \mathbf{y}_{B_{n,\epsilon}(\mathbf{x})} \mid \mathcal{D}_n) + \eta_S^2(\mathbf{x}) + \epsilon \quad (12)$$

where $B_{n,\epsilon}(\mathbf{x})$ is an ϵ -approximate Markov boundary of \mathbf{x} in \mathcal{S} .

Proof. We have

$$\begin{aligned} \sigma_n^2(\mathbf{x}) &= \text{Var}[f_{\mathbf{x}} \mid \mathcal{D}_n] - \eta_S^2(\mathbf{x}) + \eta_S^2(\mathbf{x}) \\ &\stackrel{(i)}{\leq} \text{Var}[f_{\mathbf{x}} \mid \mathcal{D}_n] - \text{Var}[f_{\mathbf{x}} \mid \mathbf{y}_{B_{n,\epsilon}(\mathbf{x})}, \mathcal{D}_n] \\ &\quad + \eta_S^2(\mathbf{x}) + \epsilon \\ &\stackrel{(ii)}{\leq} \sigma^2 \log \left(\frac{\text{Var}[f_{\mathbf{x}} \mid \mathcal{D}_n]}{\text{Var}[f_{\mathbf{x}} \mid \mathbf{y}_{B_{n,\epsilon}(\mathbf{x})}, \mathcal{D}_n]} \right) \\ &\quad + \eta_S^2(\mathbf{x}) + \epsilon \\ &= 2\sigma^2 \cdot \mathbf{I}(f_{\mathbf{x}}; \mathbf{y}_{B_{n,\epsilon}(\mathbf{x})} \mid \mathcal{D}_n) + \eta_S^2(\mathbf{x}) + \epsilon \end{aligned}$$

where (i) follows from the defining property of an ϵ -approximate Markov boundary (cf. Equation (9)); and (ii) follows from Lemma D.13 and using monotonicity of variance. \square

Lemma D.6. For any $\epsilon > 0$, $n \geq 0$, and $\mathbf{x} \in \mathcal{A}$,

$$\mathbf{I}(f_{\mathbf{x}}; \mathbf{y}_{B_{n,\epsilon}(\mathbf{x})} \mid \mathcal{D}_n) \leq b_\epsilon \Gamma_n \quad (13)$$

where $B_{n,\epsilon}(\mathbf{x})$ is an ϵ -approximate Markov boundary of \mathbf{x} in \mathcal{S} with $|B_{n,\epsilon}(\mathbf{x})| \leq b_\epsilon$.

Proof. We use the abbreviated notation $B = B_{n,\epsilon}(\mathbf{x})$. We have

$$\begin{aligned} \mathbf{I}(f_{\mathbf{x}}; \mathbf{y}_B \mid \mathcal{D}_n) &\stackrel{(i)}{\leq} \mathbf{I}(\mathbf{f}_{\mathcal{A}}; \mathbf{y}_B \mid \mathcal{D}_n) \\ &\stackrel{(ii)}{\leq} \sum_{\tilde{\mathbf{x}} \in B} \mathbf{I}(\mathbf{f}_{\mathcal{A}}; y_{\tilde{\mathbf{x}}} \mid \mathcal{D}_n) \\ &\stackrel{(iii)}{\leq} b_\epsilon \max_{\tilde{\mathbf{x}} \in B} \mathbf{I}(\mathbf{f}_{\mathcal{A}}; y_{\tilde{\mathbf{x}}} \mid \mathcal{D}_n) \\ &\stackrel{(iv)}{\leq} b_\epsilon \max_{\tilde{\mathbf{x}} \in \mathcal{S}} \mathbf{I}(\mathbf{f}_{\mathcal{A}}; y_{\tilde{\mathbf{x}}} \mid \mathcal{D}_n) \\ &= b_\epsilon \Gamma_n \end{aligned}$$

where (i) follows from monotonicity of mutual information; (ii) follows from the chain rule of information gain and the monotonicity of conditional information gain which is due to $\mathcal{D}_n \perp y_{\tilde{\mathbf{x}}} \mid \mathbf{f}_{\mathcal{A}}$ for all $\tilde{\mathbf{x}} \in B \subseteq \mathcal{S}$; (iii) follows from $b \leq b_\epsilon$; and (iv) follows from $B \subseteq \mathcal{S}$. \square

Proof of Theorem 3.1. Fix any $\mathbf{x} \in \mathcal{A}$ and $\epsilon > 0$. By Lemma D.4, there exists an ϵ -approximate Markov boundary $B_{n,\epsilon}(\mathbf{x})$ of \mathbf{x} in \mathcal{S} such that $|B_{n,\epsilon}(\mathbf{x})| \leq b_\epsilon$. We have

$$\begin{aligned} \sigma_n^2(\mathbf{x}) &\stackrel{(i)}{\leq} 2\sigma^2 \cdot \mathbf{I}(f_{\mathbf{x}}; \mathbf{y}_{B_{n,\epsilon}(\mathbf{x})} \mid \mathcal{D}_n) + \eta_S^2(\mathbf{x}) + \epsilon \\ &\stackrel{(ii)}{\leq} 2\sigma^2 b_\epsilon \Gamma_n + \eta_S^2(\mathbf{x}) + \epsilon \\ &\stackrel{(iii)}{\leq} 2\sigma^2 b_\epsilon \frac{\gamma_{n+1}}{n+1} + \eta_S^2(\mathbf{x}) + \epsilon \end{aligned}$$

where (i) follows from Lemma D.5; (ii) follows from Lemma D.6; and follows from Theorem D.1 using that **ITL** generated the sequence $\{\mathbf{x}_i\}_{i=1}^n$. The result follows by setting $C_\epsilon = 2\sigma^2 b_\epsilon$. \square

D.3.2 EXEMPLARY APPLICATION OF THEOREM 3.1

Let $\epsilon = c \frac{\gamma \sqrt{n}}{\sqrt{n}}$ with $c = 2|\mathcal{S}|^2 \sigma^4 \tilde{\sigma}^2 / \lambda_{\min}^2(\text{Var}[\mathbf{f}_{\mathcal{S}}])$. Then, by Equation (10), b_ϵ can be bounded for instance by \sqrt{n} . Together with Theorem D.1 this implies for **ITL** that

$$\begin{aligned} \nu_{n,\epsilon}^2 + \epsilon &\leq 2\sigma^2 \sqrt{n} \Gamma_n + c \gamma \sqrt{n} / \sqrt{n} \\ &\leq c' \gamma_n / \sqrt{n} \end{aligned}$$

for a constant c' , e.g., $c' = 2\sigma^2 + c$. This guarantees that the reducible uncertainty of **ITL** converges, e.g., for Gaussian and smooth Matérn kernels.

D.3.3 EXISTENCE OF AN APPROXIMATE MARKOV BOUNDARY

We now derive Lemma D.4 which shows the existence of an approximate Markov boundary of \mathbf{x} in \mathcal{S} .

Lemma D.7. *For any $k \geq 0$, there exists $B \subseteq \mathcal{S}$ with $|B| = k$ such that for all $\mathbf{x}' \in \mathcal{S}$,*

$$\text{Var}[f_{\mathbf{x}'} | \mathbf{y}_B] \leq 2\tilde{\sigma}^2 \frac{\gamma_k}{k}. \quad (14)$$

Proof. We choose $B \subseteq \mathcal{S}$ greedily using the acquisition function

$$\tilde{\mathbf{x}}_k \stackrel{\text{def}}{=} \arg \max_{\tilde{\mathbf{x}} \in \mathcal{S}} \text{I}(\mathbf{f}_{\mathcal{S}}; y_{\tilde{\mathbf{x}}} | \mathbf{y}_{B_{k-1}})$$

where $B_k = \tilde{\mathbf{x}}_{1:k}$. Note that this is the special case of **ITL** with $\mathcal{S} \subseteq \mathcal{A}$, and hence, we have

$$\begin{aligned} \text{Var}[f_{\mathbf{x}'} | \mathbf{y}_{B_k}] &\stackrel{(i)}{\leq} 2\tilde{\sigma}^2 \Gamma_k \\ &\stackrel{(ii)}{\leq} 2\tilde{\sigma}^2 \frac{\gamma_{k+1}}{k+1} \end{aligned}$$

where (i) is due to Lemma D.2; and (ii) is due to Theorem D.1 and $\alpha_k(\mathcal{S}; \mathcal{S}) \leq 1$. \square

Lemma D.8. *Given any $\epsilon > 0$ and $B \subseteq \mathcal{S}$, such that for any $\mathbf{x}' \in \mathcal{S}$,*

$$\text{Var}[f_{\mathbf{x}'} | \mathbf{y}_B] \leq \frac{\epsilon \lambda_{\min}^2(\text{Var}[\mathbf{f}_{\mathcal{S}}])}{|\mathcal{S}|^2 \sigma^4}. \quad (15)$$

Then for any $\mathbf{x} \in \mathcal{X}$,

$$\text{Var}[f_{\mathbf{x}} | \mathbf{y}_B] \leq \text{Var}[f_{\mathbf{x}} | \mathbf{f}_{\mathcal{S}}] + \epsilon. \quad (16)$$

Proof. We will denote the right-hand side of Equation (15) by ϵ' . We have

$$\begin{aligned} &\text{Var}[f_{\mathbf{x}} | \mathbf{y}_B] \\ &\stackrel{(i)}{=} \mathbb{E}_{\mathbf{f}_{\mathcal{S}}}[\text{Var}_{f_{\mathbf{x}}}[f_{\mathbf{x}} | \mathbf{f}_{\mathcal{S}}, \mathbf{y}_B] | \mathbf{y}_B] \\ &\quad + \text{Var}_{\mathbf{f}_{\mathcal{S}}}[\mathbb{E}_{f_{\mathbf{x}}}[f_{\mathbf{x}} | \mathbf{f}_{\mathcal{S}}, \mathbf{y}_B] | \mathbf{y}_B] \\ &\stackrel{(ii)}{=} \text{Var}_{f_{\mathbf{x}}}[f_{\mathbf{x}} | \mathbf{f}_{\mathcal{S}}, \mathbf{y}_B] + \text{Var}_{\mathbf{f}_{\mathcal{S}}}[\mathbb{E}_{f_{\mathbf{x}}}[f_{\mathbf{x}} | \mathbf{f}_{\mathcal{S}}, \mathbf{y}_B] | \mathbf{y}_B] \\ &\stackrel{(iii)}{=} \underbrace{\text{Var}_{f_{\mathbf{x}}}[f_{\mathbf{x}} | \mathbf{f}_{\mathcal{S}}]}_{\text{irreducible uncertainty}} + \underbrace{\text{Var}_{\mathbf{f}_{\mathcal{S}}}[\mathbb{E}_{f_{\mathbf{x}}}[f_{\mathbf{x}} | \mathbf{f}_{\mathcal{S}}] | \mathbf{y}_B]}_{\text{reducible (epistemic) uncertainty}} \end{aligned}$$

where (i) follows from the law of total variance; (ii) uses that the conditional variance of a Gaussian depends only on the location of observations and not on their value; and (iii) follows from $f_{\mathbf{x}} \perp \mathbf{y}_B | \mathbf{f}_{\mathcal{S}}$ since $B \subseteq \mathcal{S}$. It remains to bound the reducible uncertainty.

Let $h : \mathbb{R}^d \rightarrow \mathbb{R}$, $\mathbf{f}_{\mathcal{S}} \mapsto \mathbb{E}[f_{\mathbf{x}} | \mathbf{f}_{\mathcal{S}}]$ where we write $d \stackrel{\text{def}}{=} |\mathcal{S}|$. Using the formula for the GP posterior mean, we have

$$h(\mathbf{f}_{\mathcal{S}}) = \mathbb{E}[f_{\mathbf{x}}] + \mathbf{z}^\top (\mathbf{f}_{\mathcal{S}} - \mathbb{E}[\mathbf{f}_{\mathcal{S}}])$$

where $\mathbf{z} \stackrel{\text{def}}{=} \mathbf{K}^{-1} \mathbf{k}$, $\mathbf{K} \stackrel{\text{def}}{=} \text{Var}[\mathbf{f}_S]$, and $\mathbf{k} \stackrel{\text{def}}{=} \text{Cov}[\mathbf{f}_S, f_{\mathbf{x}}]$. Because h is a linear function in \mathbf{f}_S we have for the reducible uncertainty that

$$\begin{aligned} \text{Var}_{\mathbf{f}_S}[h(\mathbf{f}_S) \mid \mathbf{y}_B] &= \mathbf{z}^\top \text{Var}[\mathbf{f}_S \mid \mathbf{y}_B] \mathbf{z} \\ &\stackrel{(i)}{\leq} d \cdot \mathbf{z}^\top \text{diag}\{\text{Var}[f_{\mathbf{x}'} \mid \mathbf{y}_B]\} \mathbf{z} \\ &\stackrel{(ii)}{\leq} \epsilon' d \|\mathbf{z}\|_2^2 \\ &= \epsilon' d \|\mathbf{K}^{-1} \mathbf{k}\|_2^2 \\ &\leq \epsilon' d \|\mathbf{K}^{-1}\|_2^2 \|\mathbf{k}\|_2^2 \\ &= \frac{\epsilon' d \|\mathbf{k}\|_2^2}{\lambda_{\min}^2(\mathbf{K})} \end{aligned}$$

where (i) follows from Lemma D.12; and (ii) follows from the assumption that $\text{Var}[f_{\mathbf{x}'} \mid \mathbf{y}_B] \leq \epsilon'$ for all $\mathbf{x}' \in S$. We have

$$\|\mathbf{k}\|_2^2 = \sum_{\mathbf{x}' \in S} \underbrace{\text{Cov}[f_{\mathbf{x}}, f_{\mathbf{x}'}]^2}_{\leq \sigma^4} \leq d\sigma^4.$$

Thus,

$$\text{Var}_{\mathbf{f}_S}[h(\mathbf{f}_S) \mid \mathbf{y}_B] \leq \frac{\epsilon' d^2 \sigma^4}{\lambda_{\min}^2(\mathbf{K})} = \epsilon.$$

□

Proof of Lemma D.4. Let B be the set of size k generated by Lemma D.7 to satisfy $\text{Var}[f_{\mathbf{x}'} \mid \mathbf{y}_B] \leq 2\tilde{\sigma}^2 \gamma_k / k$ for all $\mathbf{x}' \in S$. We have for any $\mathbf{x} \in \mathcal{X}$,

$$\begin{aligned} \text{Var}[f_{\mathbf{x}} \mid \mathcal{D}_n, \mathbf{y}_B] &\stackrel{(i)}{\leq} \text{Var}[f_{\mathbf{x}} \mid \mathbf{y}_B] \\ &\stackrel{(ii)}{\leq} \text{Var}[f_{\mathbf{x}} \mid \mathbf{f}_S] + \epsilon \end{aligned}$$

where (i) follows from monotonicity of variance; and (ii) follows from Lemma D.8 and using the condition on k . □

We remark that Lemma D.7 provides an algorithm (just “undirected” **ITL**!) to compute an approximate Markov boundary, and the set B returned by this algorithm is a valid approximate Markov boundary for all $\mathbf{x} \in \mathcal{X}$.

D.4 PROOF OF THEOREM 3.2

We first formalize the assumptions of Theorem 3.2:

Assumption D.9 (Regularity of f^*). We assume that f^* is in a reproducing kernel Hilbert space $\mathcal{H}_k(\mathcal{X})$ associated with a kernel k and has bounded norm, that is, $\|f\|_k \leq B$ for some finite $B \in \mathbb{R}$.

Assumption D.10 (Sub-Gaussian noise). We further assume that each ϵ_n from the noise sequence $\{\epsilon_n\}_{n=1}^\infty$ is conditionally zero-mean $\rho(\mathbf{x}_n)$ -sub-Gaussian with known constants $\rho(\mathbf{x}) > 0$ for all $\mathbf{x} \in \mathcal{X}$. Concretely,

$$\forall n \geq 1, \lambda \in \mathbb{R} : \quad \mathbb{E}[e^{\lambda \epsilon_n} \mid \mathcal{D}_{n-1}] \leq \exp\left(\frac{\lambda^2 \rho^2(\mathbf{x}_n)}{2}\right)$$

where \mathcal{D}_{n-1} corresponds to the σ -algebra generated by the random variables $\{\mathbf{x}_i, \epsilon_i\}_{i=1}^{n-1}$ and \mathbf{x}_n .

We make use of the following foundational result, showing that under the above two assumptions the (misspecified) Gaussian process model from Section 3.1 is an all-time well-calibrated model of f^* :

Lemma D.11 (Well-calibrated confidence intervals; Abbasi-Yadkori (2013); Chowdhury & Gopalan (2017)). *Pick $\delta \in (0, 1)$ and let Assumptions D.9 and D.10 hold. Let*

$$\beta_n(\delta) = \beta_n(\delta) = \|f^*\|_k + \rho\sqrt{2(\gamma_n + 1 + \log(1/\delta))}$$

where $\rho = \max_{\mathbf{x} \in \mathcal{X}} \rho(\mathbf{x})$.¹³ Then, for all $\mathbf{x} \in \mathcal{X}$ and $n \geq 0$ jointly with probability at least $1 - \delta$,

$$|f^*(\mathbf{x}) - \mu_n(\mathbf{x})| \leq \beta_n(\delta) \cdot \sigma_n(\mathbf{x})$$

where $\mu_n(\mathbf{x})$ and $\sigma_n^2(\mathbf{x})$ are mean and variance (as defined in Appendix B.2) of the GP posterior of $f(\mathbf{x})$ conditional on the observations \mathcal{D}_n , pretending that ε_i is Gaussian with variance $\rho^2(\mathbf{x}_i)$.

The proof of Theorem 3.2 is a straightforward application of Lemma D.11 and Theorem 3.1:

Proof of Theorem 3.2. By Theorem 3.1, we have that for all $\mathbf{x} \in \mathcal{A}$,

$$\sigma_n(\mathbf{x}) \leq \sqrt{\eta_S^2(\mathbf{x}) + \nu_{n,\epsilon^2}^2 + \epsilon^2} \leq \eta_S(\mathbf{x}) + \nu_{n,\epsilon^2} + \epsilon.$$

The result then follows by application of Lemma D.11. \square

D.5 USEFUL FACTS AND INEQUALITIES

We denote by \preceq the Loewner partial ordering of symmetric matrices.

Lemma D.12. *Let $\mathbf{A} \in \mathbb{R}^{n \times n}$ be a positive definite matrix with diagonal \mathbf{D} . Then, $\mathbf{A} \preceq n\mathbf{D}$.*

Proof. Equivalently, one can show $n\mathbf{D} - \mathbf{A} \succeq \mathbf{0}$. We write $\mathbf{A} \stackrel{\text{def}}{=} \mathbf{D}^{1/2} \mathbf{Q} \mathbf{D}^{1/2}$, and thus, $\mathbf{Q} = \mathbf{D}^{-1/2} \mathbf{A} \mathbf{D}^{-1/2}$ is a positive definite symmetric matrix with all diagonal elements equal to 1. It remains to show that

$$n\mathbf{D} - \mathbf{A} = \mathbf{D}^{1/2}(n\mathbf{I} - \mathbf{Q})\mathbf{D}^{1/2} \succeq \mathbf{0}.$$

Note that $\sum_{i=1}^n \lambda_i(\mathbf{Q}) = \text{tr } \mathbf{Q} = n$, and hence, all eigenvalues of \mathbf{Q} belong to $(0, n)$. \square

Lemma D.13. *If $a, b \in (0, M]$ for some $M > 0$ and $b \geq a$ then*

$$b - a \leq M \cdot \log\left(\frac{b}{a}\right). \quad (17)$$

If additionally, $a \geq M'$ for some $M' > 0$ then

$$b - a \geq M' \cdot \log\left(\frac{b}{a}\right). \quad (18)$$

Proof. Let $f(x) \stackrel{\text{def}}{=} \log x$. By the mean value theorem, there exists $c \in (a, b)$ such that

$$\frac{1}{c} = f'(c) = \frac{f(b) - f(a)}{b - a} = \frac{\log b - \log a}{b - a} = \frac{\log(\frac{b}{a})}{b - a}.$$

Thus,

$$b - a = c \cdot \log\left(\frac{b}{a}\right) < M \cdot \log\left(\frac{b}{a}\right).$$

Under the additional condition that $a \geq M'$, we obtain

$$b - a = c \cdot \log\left(\frac{b}{a}\right) > M' \cdot \log\left(\frac{b}{a}\right).$$

\square

¹³ $\beta_n(\delta)$ can be tightened adaptively (Emmenegger et al., 2023).

E CORRELATION-BASED TRANSDUCTIVE LEARNING

We will briefly look at the decision rule

$$\mathbf{x}_n = \arg \max_{\mathbf{x} \in \mathcal{S}} \sum_{\mathbf{x}' \in \mathcal{A}} \text{Cor}[f_{\mathbf{x}}, f_{\mathbf{x}'} \mid \mathcal{D}_{n-1}] \quad (19)$$

which as we will see can be thought of as loose approximation to **ITL**. We refer to this decision rule as **CTL**, short for *correlation-based transductive learning*.

We consider the GP setting, i.e., Assumptions B.1 and B.2 hold.

Approximation of ITL The **ITL** objective can be shown to be lower bounded by

$$\begin{aligned} \mathcal{I}(f_{\mathcal{A}}; y_{\mathcal{X}} \mid \mathcal{D}_{n-1}) &\stackrel{(i)}{\geq} \frac{1}{|\mathcal{A}|} \sum_{\mathbf{x}' \in \mathcal{A}} \mathcal{I}(f_{\mathbf{x}'}; y_{\mathcal{X}} \mid \mathcal{D}_{n-1}) \\ &\stackrel{(ii)}{=} -\frac{1}{2|\mathcal{A}|} \sum_{\mathbf{x}' \in \mathcal{A}} \log(1 - \text{Cor}[f_{\mathbf{x}'}, y_{\mathcal{X}} \mid \mathcal{D}_{n-1}]^2) \\ &\stackrel{(iii)}{\gtrsim} \sum_{\mathbf{x}' \in \mathcal{A}} \text{Cor}[f_{\mathbf{x}'}, y_{\mathcal{X}} \mid \mathcal{D}_{n-1}]^2 + \text{const} \end{aligned}$$

where (ii) is detailed in example 8.5.1 of (Cover, 1999); and (iii) follows from Jensen’s inequality and exponentiating. (i) is a loose approximation which highlights that **ITL** takes into account the correlations *between* points in \mathcal{A} while **CTL** does not.

F SUBSAMPLING TARGET SPACES

When the target space \mathcal{A} is large, it may be computationally infeasible to compute the exact objective. A natural approach to address this issue is to approximate the target space by a smaller set of size K .

One possibility is to select the K “most explanatory” points within \mathcal{A} . This selection problem is similar to the batch selection problem in active learning (Holzmüller et al., 2023) and can be tackled using, e.g., the *greedy max determinant* or *greedy max kernel distance* strategies. In the remainder of this section, we study an alternative approach which is based on sampling points from \mathcal{A} according to some probability distribution $\mathcal{P}_{\mathcal{A}}$ supported on \mathcal{A} .

F.1 STOCHASTIC TARGET SPACES

Concretely, in iteration n , a subset A of K points is sampled independently from \mathcal{A} according to the distribution $\mathcal{P}_{\mathcal{A}}$ and the objective is computed on this subset. Formally, this amounts to a single-sample Monte Carlo approximation of

$$\mathbf{x}_n \in \arg \max_{\mathbf{x} \in \mathcal{S}} \mathbb{E}_{A \sim \mathcal{P}_{\mathcal{A}}} [\mathcal{I}(f_{\mathcal{A}}; y_{\mathcal{X}} \mid \mathcal{D}_{n-1})]. \quad (20)$$

It is straightforward to extend the convergence guarantees to the setting of stochastic target spaces. Intuitively, after sufficiently many iterations, each $\mathbf{x} \in \mathcal{A}$ will have been sampled roughly as often as its “weight” (i.e., probability) suggests.

Lemma F.1. *Consider the stochastic target space setting. For any $n \geq 0$, $K \geq 1$, and $\mathbf{x} \in \mathcal{A}$, with probability at least $1 - \exp(-n\nu/8)$ where $\nu = 1 - (1 - \mathcal{P}_{\mathcal{A}}(\mathbf{x}))^K$, we have that after at most n iterations \mathbf{x} was within the subsampled target space in at least $n\nu/2$ iterations.*

Proof. Let $Y_i \sim \text{Binom}(K, \mathcal{P}_{\mathcal{A}}(\mathbf{x}))$ denote the random variable counting the number of occurrences of \mathbf{x} in \mathcal{A}'_i . Moreover, we write $X_i \stackrel{\text{def}}{=} \mathbb{1}\{\mathbf{x} \in \mathcal{A}'_i\}$. Note that

$$\begin{aligned} \nu_i &\stackrel{\text{def}}{=} \mathbb{E} X_i = \mathbb{P}(\mathbf{x} \in \mathcal{A}'_i) \\ &= 1 - \mathbb{P}(Y_i = 0) \\ &= 1 - (1 - \mathcal{P}_{\mathcal{A}}(\mathbf{x}))^K \end{aligned}$$

$$= \nu.$$

Let $X \stackrel{\text{def}}{=} \sum_{i=1}^n X_i$ with $\mathbb{E}X = n\nu$. By Chernoff’s bound,

$$\mathbb{P}\left(X \leq \frac{n\nu}{2}\right) \leq \exp\left(-\frac{n\nu}{8}\right).$$

□

With this result, the previously derived convergence guarantees follow also for the stochastic target space setting. We leave a tighter analysis of stochastic target spaces to future work.

G COMPUTATIONAL COMPLEXITY

Evaluating the acquisition function of **ITL** in round n requires computing for each $\mathbf{x} \in \mathcal{S}$,

$$\begin{aligned} I(\mathbf{f}_{\mathcal{A}}; y_{\mathbf{x}} \mid \mathcal{D}_n) &= \frac{1}{2} \log \left(\frac{|\text{Var}[\mathbf{f}_{\mathcal{A}} \mid \mathcal{D}_n]|}{|\text{Var}[\mathbf{f}_{\mathcal{A}} \mid y_{\mathbf{x}}, \mathcal{D}_n]|} \right) && \text{(forward)} \\ &= \frac{1}{2} \log \left(\frac{\text{Var}[y_{\mathbf{x}} \mid \mathcal{D}_n]}{\text{Var}[y_{\mathbf{x}} \mid \mathbf{f}_{\mathcal{A}}, \mathcal{D}_n]} \right) && \text{(backward)}. \end{aligned}$$

Let $|\mathcal{S}| = m$ and $|\mathcal{A}| = k$. Then, the forward method has complexity $O(m \cdot k^3)$. For the backward method, observe that the variances are scalar and the covariance matrix $\text{Var}[\mathbf{f}_{\mathcal{A}} \mid \mathcal{D}_n]$ only has to be inverted once for all points \mathbf{x} . Thus, the backward method has complexity $O(k^3 + m)$.

When the size m of \mathcal{S} is relatively small (and hence, all points in \mathcal{S} can be considered during each iteration of the algorithm), GP inference corresponds simply to computing conditional distributions of a multivariate Gaussian. The performance can therefore be improved by keeping track of the full posterior distribution over $\mathbf{f}_{\mathcal{S}}$ of size $O(m^2)$ and conditioning on the latest observation during each iteration of the algorithm. In this case, after each observation the posterior can be updated at a cost of $O(m^2)$ which does not grow with the time n , unlike classical GP inference.

Overall, when m is small, the computational complexity of **ITL** is $O(k^3 + m^2)$. When m is large (or possibly infinite) and a subset of \tilde{m} points is considered in a given iteration, the computational complexity of **ITL** is $O(k^3 + \tilde{m} \cdot n^3)$, neglecting the complexity of selecting the \tilde{m} candidate points. In the latter case, the computational cost of **ITL** is dominated by the cost of GP inference.

Khanna et al. (2017) discuss distributed and stochastic approximations of greedy algorithms to (weakly) submodular problems that are also applicable to **ITL**.

H ADDITIONAL NN EXPERIMENTS & DETAILS

We outline the few-shot training of NNs in Algorithm 1.

In Appendix H.1, we detail metrics and hyperparameters. We describe in Appendices H.2 and H.3 how to compute the (initial) conditional kernel matrix \mathbf{K} , and in Appendix H.4 how to update this matrix \mathbf{K} to obtain conditional embeddings for batch selection.

In Appendix H.5, we show that **ITL** and **CTL** significantly outperform a wide selection of commonly used heuristics. In Appendices H.6 and H.7, we conduct additional experiments and ablations.

Hübötter et al. (2024) provides additional comparisons with respect to a variance-based transductive decision rule.

H.1 EXPERIMENT DETAILS

We evaluate the accuracy with respect to $\mathcal{P}_{\mathcal{A}}$ using a Monte Carlo approximation with out-of-sample data:

$$\text{accuracy}(\hat{\boldsymbol{\theta}}) \approx \mathbb{E}_{(\mathbf{x}, y) \sim \mathcal{P}_{\mathcal{A}}} \mathbb{1}\{y = \arg \max_i f_i(\mathbf{x}; \hat{\boldsymbol{\theta}})\}.$$

Algorithm 1 Few-shot training of NNs

Given: initialized or pre-trained model f , *small* sample $A \sim \mathcal{P}_A$
initialize dataset $\mathcal{D} = \emptyset$
repeat
 sample $S \sim \mathcal{P}_S$
 subsample target space $A' \stackrel{\text{u.a.r.}}{\sim} A$
 initialize batch $B = \emptyset$
 compute kernel matrix \mathbf{K} over domain $[S, A']$
 repeat b **times**
 compute acquisition function w.r.t. A' , based on \mathbf{K}
 add maximizer $x \in S$ of acquisition function to B
 update conditional kernel matrix \mathbf{K}
 obtain labels for B and add to dataset \mathcal{D}
 update f using data \mathcal{D}

Table 1: Hyperparameter summary of NN experiments. (*) we train until convergence on oracle validation accuracy.

	MNIST	CIFAR-100
ρ	0.01	1
M	30	100
m	3	10
k	1 000	1 000
batch size b	1	10
# of epochs	(*)	5
learning rate	0.001	0.001

We provide an overview of the hyperparameters used in our NN experiments in Table 1. The effect of noise standard deviation ρ is small for all tested $\rho \in [1, 100]$ (cf. ablation study in Table 2).¹⁴ M denotes the size of the sample $A \sim \mathcal{P}_A$. In each iteration, we select the target space $\mathcal{A} \leftarrow A'$ as a random subset of m points from A .¹⁵ We provide an ablation over m in Appendix H.6.

During each iteration, we select the batch B according to the decision rule from a random sample from \mathcal{P}_S of size k .¹⁶

Since we train the MNIST model from scratch, we train from random initialization until convergence on oracle validation accuracy.¹⁷ We do this to stabilize the learning curves, and provide the least biased (due to the training algorithm) results. For CIFAR-100, we train for 5 epochs (starting from the previous iterations' model) which we found to be sufficient to obtain good performance.

We use the ADAM optimizer (Kingma & Ba, 2014). In our CIFAR-100 experiments, we use a pre-trained EfficientNet-B0 (Tan & Le, 2019), and fine-tune the final and penultimate layers. We freeze earlier layers to prevent overfitting to the few-shot training data.

To prevent numerical inaccuracies when computing the **ITL** objective, we optimize

$$I(\mathbf{y}_A; y_x \mid \mathcal{D}_{n-1}) = \frac{1}{2} \log \left(\frac{\text{Var}[y_x \mid \mathcal{D}_{n-1}]}{\text{Var}[y_x \mid \mathbf{y}_A, \mathcal{D}_{n-1}]} \right) \quad (21)$$

¹⁴We use a larger noise standard deviation ρ in CIFAR-100 to stabilize the numerics of batch selection via conditional embeddings (cf. Table 2).

¹⁵This appears to improve the training, likely because it prevents overfitting to peculiarities in the finite sample A (cf. Figure 10).

¹⁶In large-scale problems, the work of Coleman et al. (2022) suggests to use an (approximate) nearest neighbor search to select the (large) candidate set rather than sampling u.a.r. from \mathcal{P}_S . This can be a viable alternative to simply increasing k and suggests future work.

¹⁷That is, to stop training as soon as accuracy on a validation set from \mathcal{P}_A decreases in an epoch.

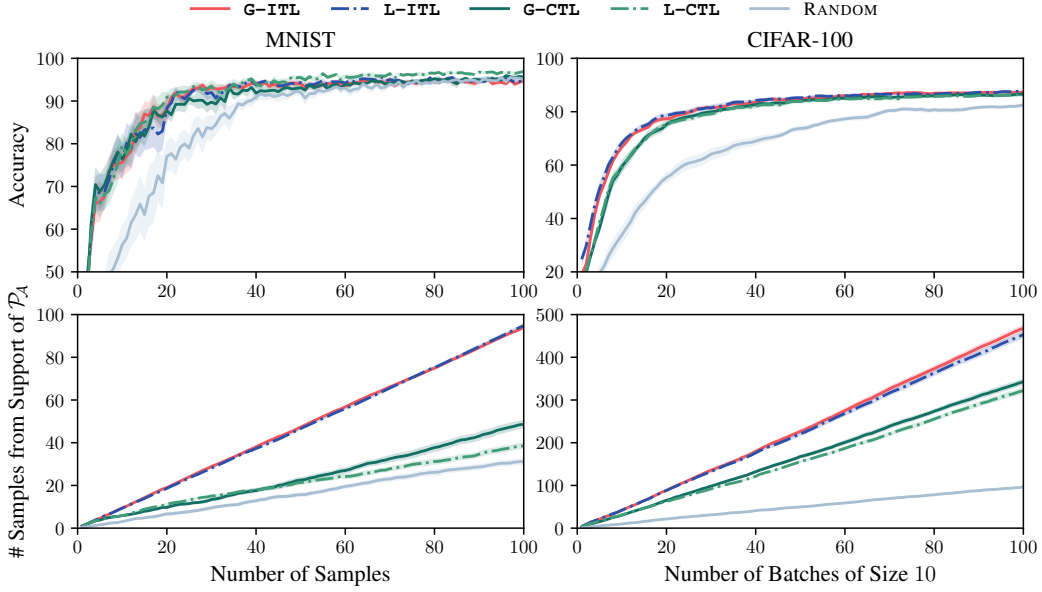


Figure 4: Comparison of loss gradient (“G-”) and last-layer embeddings (“L-”).

instead of Equation (1), which amounts to adding ρ^2 to the diagonal of the covariance matrix before inversion. This appears to improve numerical stability, especially when using gradient embeddings.¹⁸

H.2 EMBEDDINGS AND KERNELS

Using a neural network to parameterize f , we evaluate the canonical approximations of f by a stochastic process in the following.

An embedding $\phi(x)$ is a latent representation of an input x . Collecting the embeddings as rows in the design matrix Φ of a set of inputs X , one can approximate the network by the linear function $f_X = \Phi\beta$ with weights β . Approximating the weights by $\beta \sim \mathcal{N}(\mu, \Sigma)$ implies that $f_X \sim \mathcal{N}(\Phi\mu, \Phi\Sigma\Phi^\top)$. The covariance matrix $K_{XX} = \Phi\Sigma\Phi^\top$ can be succinctly represented in terms of its associated kernel $k(x, x') = \phi(x)^\top \Sigma \phi(x')$. Here,

- $\phi(x)$ is the latent representation of x , and
- Σ captures the dependencies in the latent space.

While any choice of embedding ϕ is possible, the following are common choices:

1. *Last-Layer*: A common choice for $\phi(x)$ is the representation of x from the penultimate layer of the neural network (Holzmüller et al., 2023). Interpreting the early layers as a feature encoder, this uses the low-dimensional feature map akin to random feature methods (Rahimi & Recht, 2007).
2. *Output Gradients (empirical NTK)*: Another common choice is $\phi(x) = \nabla_{\theta} f(x; \theta)$ where θ are the network parameters (Holzmüller et al., 2023). Its associated kernel is known as the (empirical) *neural tangent kernel* (NTK) and the posterior mean of this GP approximates wide NNs trained with gradient descent (Arora et al., 2019; Khan et al., 2019; He et al., 2020). Kassraie & Krause (2022) derive bounds of γ_n under this kernel. If θ is restricted to the weights of the final linear layer, then this embedding is simply the last-layer embedding.
3. *Loss Gradients*: Another possible choice is

$$\phi(x) = \nabla_{\theta} \ell(f(x; \theta), \hat{y}(x))|_{\theta=\hat{\theta}}$$

¹⁸In our experiments, we observe that the effect of various choices of ρ on this slight adaptation of the **ITL** decision rule has negligible impact on performance. The more prominent effect of ρ appears to arise from the batch selection via conditional embeddings (cf. Table 2).

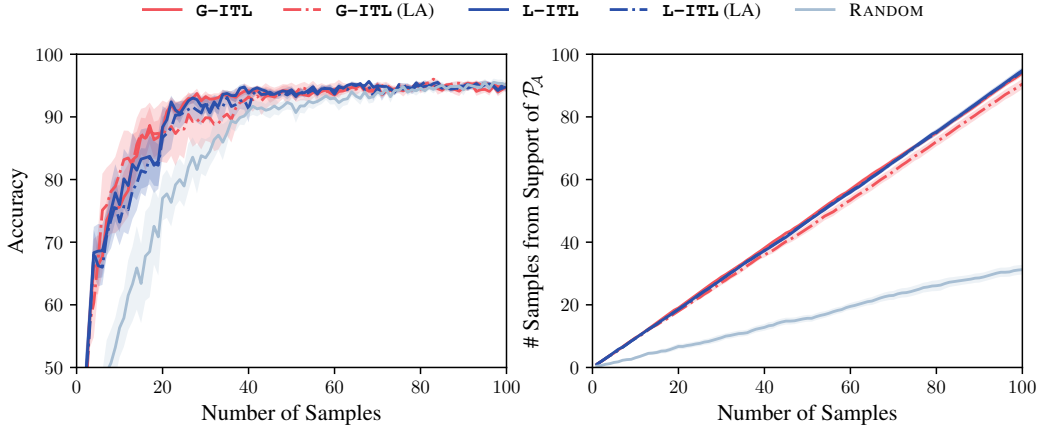


Figure 5: Uncertainty quantification (i.e., estimation of Σ) via a Laplace approximation (LA, Daxberger et al. (2021)) over last-layer weights using a Kronecker factored log-likelihood Hessian approximation (Martens & Grosse, 2015) and the loss gradient embeddings from Equation (22). The results are shown for the MNIST experiment. We do not observe a performance improvement beyond the trivial approximation $\Sigma = \mathbf{I}$.

where ℓ is a loss function, $\hat{y}(\mathbf{x})$ is the predicted label, and $\hat{\theta}$ are the current parameter estimates Ash et al. (2020).

4. *Outputs (empirical NNGP)*: Another possible choice is $\phi(\mathbf{x}) = \mathbf{f}(\mathbf{x})$, i.e., the output of the network. Its associated kernel is known as the (empirical) *neural network Gaussian process* (NNGP) kernel (Lee et al., 2018).

In the additional experiments from this appendix we use last-layer embeddings unless noted otherwise. We compare the performance of last-layer and the loss gradient embedding

$$\phi(\mathbf{x}) = \nabla_{\theta'} \ell_{\text{CE}}(\mathbf{f}(\mathbf{x}; \theta), \hat{y}(\mathbf{x}))|_{\theta=\hat{\theta}} \quad (22)$$

where θ' are the parameters of the final output layer, $\hat{\theta}$ are the current parameter estimates, $\hat{y}(\mathbf{x}) = \arg \max_i f_i(\mathbf{x}; \theta)$ are the associated predicted labels, and ℓ_{CE} denotes the cross-entropy loss. This gradient embedding captures the potential update direction upon observing a new point (Ash et al., 2020). Moreover, Ash et al. (2020) show that for most neural networks, the norm of these gradient embeddings are a conservative lower bound to the norm assumed by taking any other proxy label $\hat{y}(\mathbf{x})$. In Figure 4, we observe only negligible differences in performance between this and the last-layer embedding.

H.3 TOWARDS UNCERTAINTY QUANTIFICATION IN LATENT SPACE

A straightforward and common approximation of the uncertainty about NN weights is given by $\Sigma = \mathbf{I}$, and we use this approximation throughout our experiments.

The poor performance of UNSA (cf. Appendix H.5) with this approximation suggests that with more sophisticated approximations, the performance of **ITL** and **CTL** can be further improved. Further research is needed to study the effect of more sophisticated approximations of “uncertainty” in the latent space. For example, with parameter gradient embeddings, the latent space is the network parameter space where various approximations of Σ based on Laplace approximation (Daxberger et al., 2021; Antorán et al., 2022), variational inference (Blundell et al., 2015), or Markov chain Monte Carlo (Maddox et al., 2019) have been studied. We also evaluate Laplace approximation (LA, Daxberger et al. (2021)) for estimating Σ but see no improvement (cf. Figure 5). Nevertheless, we believe that uncertainty quantification is a promising direction for future work, with the potential to improve performance of **ITL** and its variations substantially.

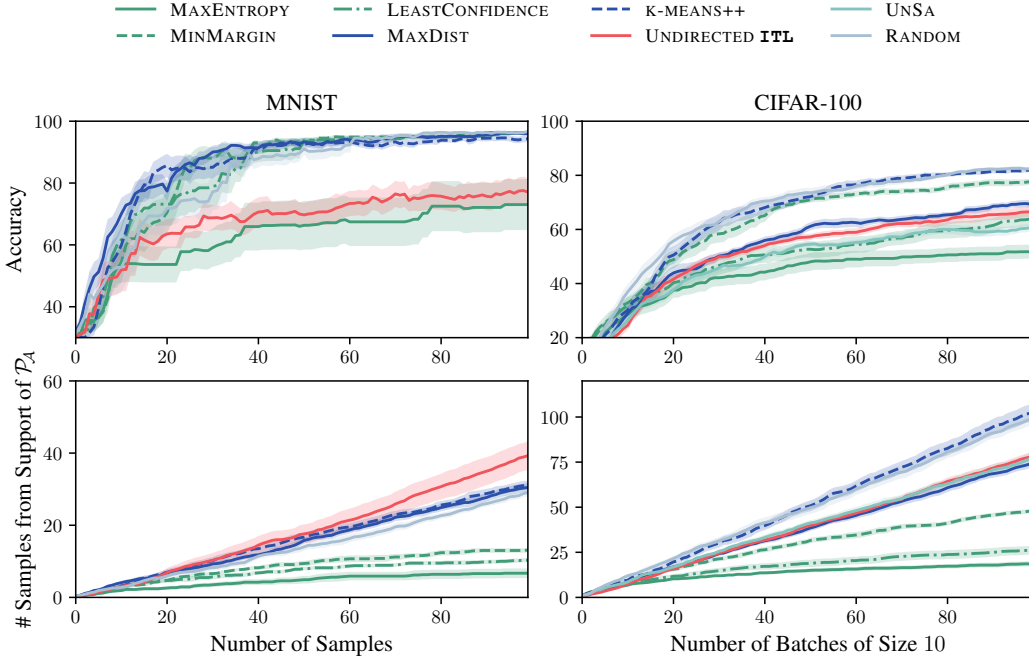


Figure 6: Comparison of “undirected” baselines for the experiment of Figure 2. In the MNIST experiment, UNSA and UNDIRECTED **ITL** coincide, and we therefore only plot the latter.

H.4 BATCH SELECTION VIA CONDITIONAL EMBEDDINGS

We will refer to Equation (4) as BACE, short for *batch selection via conditional embeddings*. BACE can be implemented efficiently using the Gaussian approximation of f_X from Appendix H.2 by iteratively conditioning on the previously selected points $x_{n,1:i-1}$, and updating the kernel matrix K_{XX} using the closed-form formula for the variance of conditional Gaussians:

$$K_{XX} \leftarrow K_{XX} - \frac{1}{K_{x_j x_j} + \rho^2} K_{X x_j} K_{x_j X} \quad (23)$$

where j denotes the index of the selected $x_{n,i}$ within X and ρ^2 is the noise variance. Note that $K_{x_j x_j}$ is a scalar and $K_{X x_j}$ is a row vector, and hence, this iterative update can be implemented efficiently.

We remark that Equations (3) and (4) are natural extensions of previous non-adaptive active learning methods, which typically maximize some notion of “distance” between points in the batch, to the “directed” setting (Ash et al., 2020; Zanette et al., 2021; Holzmüller et al., 2023; Pacchiano et al., 2024). BACE simultaneously maximizes “distance” between points in a batch and minimizes “distance” to points in \mathcal{A} .

Computational complexity of BACE As derived in Appendix G, a single batch selection step of BACE has complexity $O(b(k^3 + m^2))$ where b is the size of the batch, $k = |\mathcal{A}|$ is the size of the target space, and $m = |\mathcal{S}|$ is the size of the candidate set. In the case of large m , an alternative implementation whose runtime does not depend on m is described in Appendix G.

H.5 BASELINES

In the following, we briefly describe the most commonly used “undirected” decision rules.

Denote the softmax distribution over labels i at inputs x by

$$p_i(x; \hat{\theta}) \propto \exp(f_i(x; \hat{\theta})).$$

The following heuristics computed based on the softmax distribution aim to quantify the “uncertainty” about a particular input x :

- MAXENTROPY (Settles & Craven, 2008):

$$\mathbf{x}_n = \arg \max_{\mathbf{x} \in \mathcal{S}} H[p(\mathbf{x}; \hat{\boldsymbol{\theta}}_{n-1})].$$

- MAXMARGIN (Scheffer et al., 2001; Settles & Craven, 2008):

$$\mathbf{x}_n = \arg \min_{\mathbf{x} \in \mathcal{S}} p_1(\mathbf{x}; \hat{\boldsymbol{\theta}}_{n-1}) - p_2(\mathbf{x}; \hat{\boldsymbol{\theta}}_{n-1})$$

where p_1 and p_2 are the two largest class probabilities.

- LEASTCONFIDENCE (Lewis & Gale, 1994; Settles & Craven, 2008; Hendrycks & Gimpel, 2017; Tamkin et al., 2022):

$$\mathbf{x}_n = \arg \min_{\mathbf{x} \in \mathcal{S}} p_1(\mathbf{x}; \hat{\boldsymbol{\theta}}_{n-1})$$

where p_1 is the largest class probability.

An alternative class of decision rules aims to select diverse batches by maximizing the distances between points. Embeddings $\phi(\mathbf{x})$ induce the (Euclidean) embedding distance

$$d_\phi(\mathbf{x}, \mathbf{x}') \stackrel{\text{def}}{=} \|\phi(\mathbf{x}) - \phi(\mathbf{x}')\|_2.$$

Similarly, a kernel k induces the kernel distance

$$d_k(\mathbf{x}, \mathbf{x}') \stackrel{\text{def}}{=} \sqrt{k(\mathbf{x}, \mathbf{x}) + k(\mathbf{x}', \mathbf{x}') - 2k(\mathbf{x}, \mathbf{x}')}.$$

It is straightforward to see that if $k(\mathbf{x}, \mathbf{x}') = \phi(\mathbf{x})^\top \phi(\mathbf{x}')$, then embedding and kernel distances coincide, i.e., $d_\phi(\mathbf{x}, \mathbf{x}') = d_k(\mathbf{x}, \mathbf{x}')$.

- MAXDIST (Holzmüller et al., 2023; Yu & Kim, 2010; Sener & Savarese, 2017; Geifman & El-Yaniv, 2017) constructs the batch by choosing the point with the maximum distance to the nearest previously selected point:

$$\mathbf{x}_n = \arg \max_{\mathbf{x} \in \mathcal{S}} \min_{i < n} d(\mathbf{x}, \mathbf{x}_i)$$

- Similarly, K-MEANS++ (Holzmüller et al., 2023) selects the batch via K-MEANS++ seeding (Arthur et al., 2007; Ostrovsky et al., 2013). That is, the first centroid \mathbf{x}_1 is chosen uniformly at random and the subsequent centroids are chosen with a probability proportional to the square of the distance to the nearest previously selected centroid:

$$\mathbb{P}(\mathbf{x}_n = \mathbf{x}) \propto \min_{i < n} d(\mathbf{x}, \mathbf{x}_i)^2.$$

When using the loss gradient embeddings from Equation (22), this decision rule is known as BADGE (Ash et al., 2020).

Finally, we summarize common kernel-based decision rules.

- UNDIRECTED **ITL** chooses

$$\begin{aligned} \mathbf{x}_n &= \arg \max_{\mathbf{x} \in \mathcal{S}} I(\mathbf{f}_{\mathcal{S}}; y_{\mathbf{x}} \mid \mathcal{D}_{n-1}) \\ &= \arg \max_{\mathbf{x} \in \mathcal{S}} I(f_{\mathbf{x}}; y_{\mathbf{x}} \mid \mathcal{D}_{n-1}). \end{aligned}$$

This can be shown to be equivalent to MAXDET (Holzmüller et al., 2023) which selects

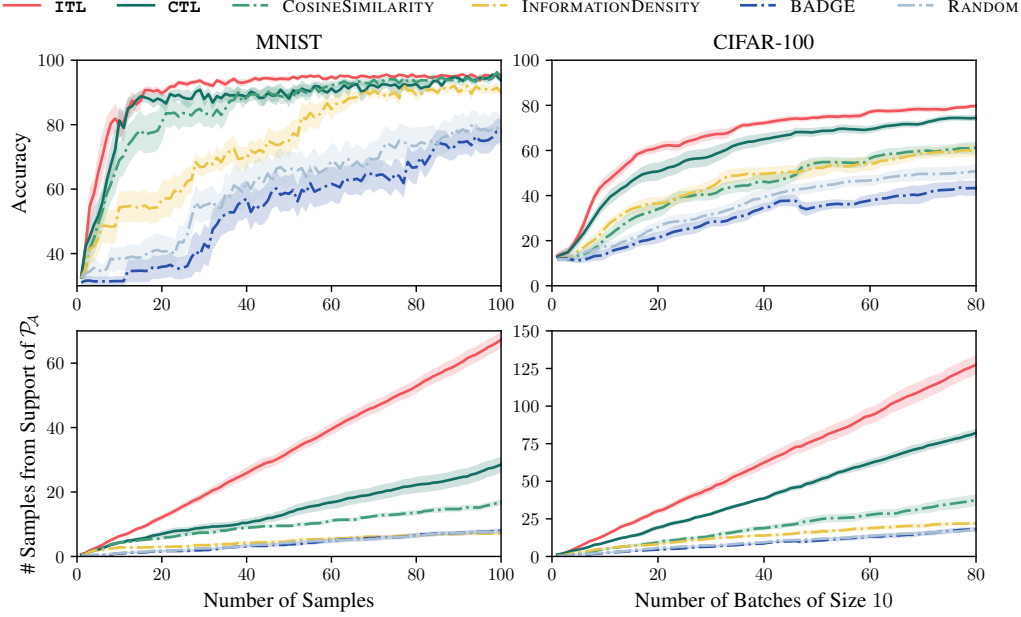
$$\mathbf{x}_n = \arg \max_{\mathbf{x} \in \mathcal{S}} |\mathbf{K}_{\mathbf{x}} + \sigma^2 \mathbf{I}|$$

where $\mathbf{K}_{\mathbf{x}}$ denotes the kernel matrix over $\mathbf{x}_{1:n-1} \cup \{\mathbf{x}\}$, conditioned on observations \mathcal{D}_{n-1} .

- Uncertainty sampling (UNSA, Lewis & Catlett, 1994) which with embeddings ϕ_{n-1} after round $n - 1$ selects:

$$\mathbf{x}_n = \arg \max_{\mathbf{x} \in \mathcal{S}} \sigma_{n-1}^2(\mathbf{x}) = \arg \max_{\mathbf{x} \in \mathcal{S}} \|\phi_{n-1}(\mathbf{x})\|_2^2.$$

With batch size $b = 1$, UNSA coincides with UNDIRECTED **ITL**. When evaluated with gradient embeddings, this acquisition function is similar to previously used “embedding length” or “gradient length” heuristics (Settles & Craven, 2008).

Figure 7: Imbalanced \mathcal{P}_S experiment.

We compare to the abovementioned decision rules and summarize the results in Figure 6. We observe that most “undirected” decision rules perform worse (and often significantly so) than RANDOM. This is likely due to frequently selecting points from the support of \mathcal{P}_S which are not in the support of \mathcal{P}_A since the points are “adversarial examples” that the model $\hat{\theta}$ is not trained to perform well on. In the case of MNIST, the poor performance can also partially be attributed to the well-known “cold-start problem” (Gao et al., 2020).

In Figure 2, we also compare to the following “directed” decision rules:

- COSINESIMILARITY (Settles & Craven, 2008) selects $\mathbf{x}_n = \arg \max_{\mathbf{x} \in \mathcal{S}} \angle_{\phi_{n-1}}(\mathbf{x}, \mathcal{A})$ where

$$\angle_{\phi}(\mathbf{x}, \mathcal{A}) \stackrel{\text{def}}{=} \frac{1}{|\mathcal{A}|} \sum_{\mathbf{x}' \in \mathcal{A}} \frac{\phi(\mathbf{x})^\top \phi(\mathbf{x}')}{\|\phi(\mathbf{x})\|_2 \|\phi(\mathbf{x}')\|_2}.$$

- INFORMATIONDENSITY (Settles & Craven, 2008) is defined as the multiplicative combination of MAXENTROPY and COSINESIMILARITY:

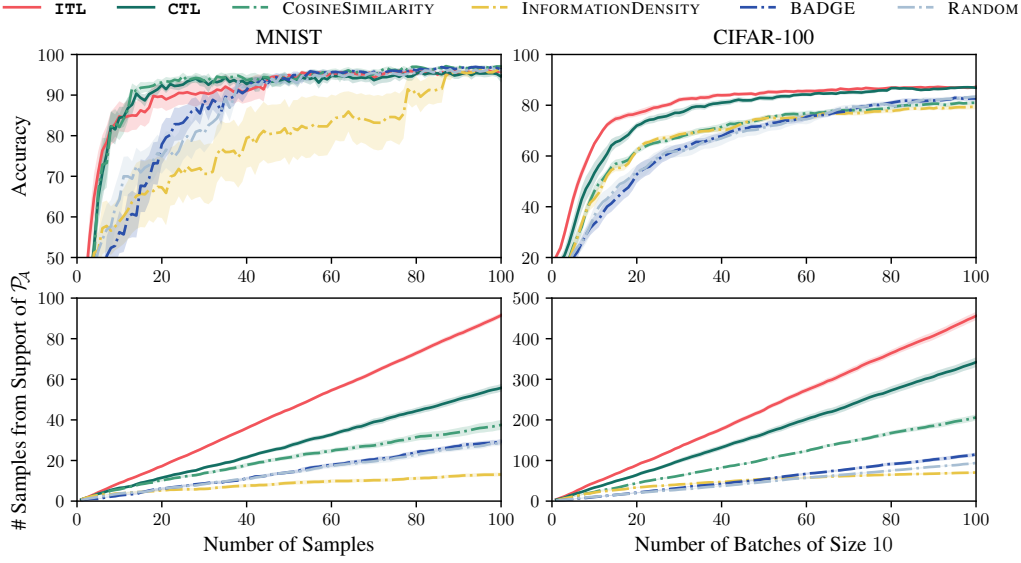
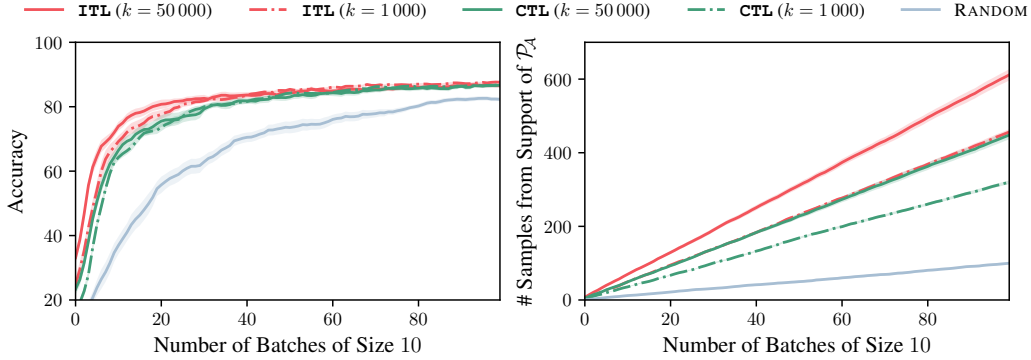
$$\mathbf{x}_n = \arg \max_{\mathbf{x} \in \mathcal{S}} H[p(\mathbf{x}; \hat{\theta}_{n-1})] \cdot \left(\angle_{\phi_{n-1}}(\mathbf{x}, \mathcal{A}) \right)^\beta$$

where $\beta > 0$ controls the relative importance of both terms. We set $\beta = 1$ in our experiments.

H.6 ADDITIONAL EXPERIMENTS

We conduct the following additional experiments:

1. *Imbalanced \mathcal{P}_S* (Figure 7): We artificially remove 80% of the support of \mathcal{P}_A from \mathcal{P}_S . For example, in case of MNIST, we remove 80% of the images with labels 3, 6, and 9 from \mathcal{P}_S . This makes the learning task more difficult, as \mathcal{P}_A is less represented in \mathcal{P}_S , meaning that the “targets” are more sparse. The trend of **ITL** outperforming **CTL** which outperforms RANDOM is even more pronounced in this setting.
2. *Imbalanced $A \sim \mathcal{P}_A$* (Figure 8): We artificially remove 50% of part of the support of \mathcal{P}_A while generating $A \sim \mathcal{P}_A$ to evaluate the robustness of **ITL** and **CTL** in presence of an imbalanced target space \mathcal{A} . Concretely, in case of MNIST, we remove 50% of the images

Figure 8: Imbalanced $A \sim \mathcal{P}_A$ experiment.Figure 9: Choice of k in the CIFAR-100 experiment.

with labels 3 and 6 from A . In case of CIFAR-100, we remove 50% of the images with labels $\{0, \dots, 4\}$ from A . We still observe the same trends as in the other experiments.

3. *Choice of k* (Figure 9): We evaluate the effect of the number of points k at which the decision rule is evaluated. Not surprisingly, we observe that the performance of **ITL** and **CTL** improves with larger k .
4. *Choice of m* (Figure 10): Next, we evaluate the choice of m , i.e., the size of the target space \mathcal{A} relative to the number M of candidate points $A \sim \mathcal{P}_A$. We write $p = m/M$. We generally observe that a larger p leads to better performance (with $p = 1$ being the best choice). However, it appears that a smaller p can be beneficial with respect to accuracy when a large number of batches are selected. We believe that this may be because a smaller p improves the diversity between selected batches.
5. *Choice of M* (Figure 11): Finally, we evaluate the choice of M , i.e., the size of $A \sim \mathcal{P}_A$. Not surprisingly, we observe that the performance of **ITL** improves with larger M .

H.7 ABLATION STUDY OF NOISE STANDARD DEVIATION ρ

In Table 2, we evaluate the CIFAR-100 experiment with different noise standard deviations ρ . We observe that the performance of batch selection via conditional embeddings drops (mostly for the less

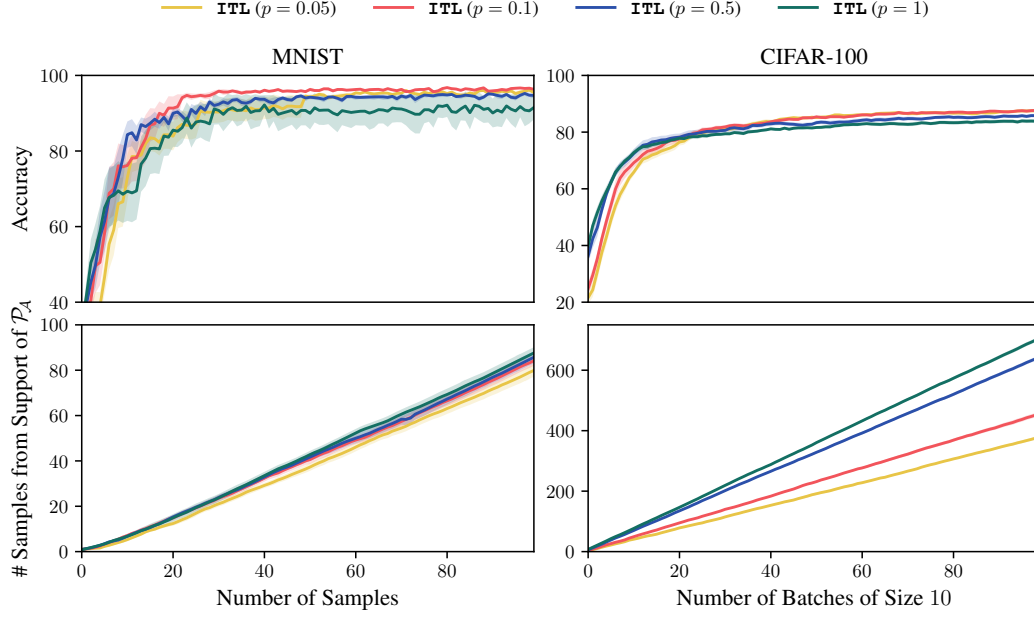


Figure 10: Evaluation of the choice of m relative to the size M of $A \sim \mathcal{P}_A$. Here, $p = m/M$.

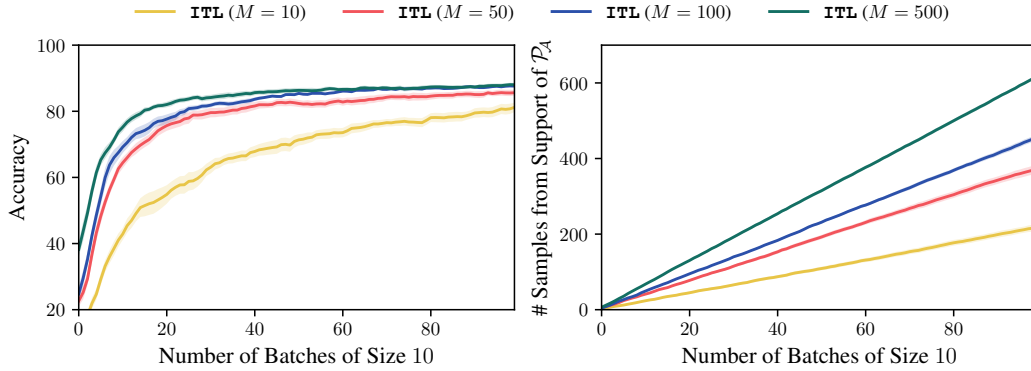


Figure 11: Evaluation of the choice of M , i.e., the size of $A \sim \mathcal{P}_A$, in the CIFAR-100 experiment.

Table 2: Ablation study of noise standard deviation ρ in the CIFAR-100 experiment. We list the accuracy after 100 rounds per decision rule, with its standard error over 10 random seeds. “(top- b)” denotes variants where batches are selected by taking the top- b points according to the decision rule rather than using batch selection via conditional embeddings. Shown in **bold** are the best performing decision rules, and shown in *italics* are results due to numerical instability.

ρ	0.0001	0.01	1	100
G-ITL	<i>78.26 ± 1.40</i>	<i>79.12 ± 1.19</i>	87.16 ± 0.29	87.18 ± 0.28
L-ITL	87.52 ± 0.48	87.52 ± 0.41	87.53 ± 0.35	86.47 ± 0.22
G-CTL	<i>58.68 ± 2.11</i>	<i>81.44 ± 1.04</i>	86.52 ± 0.44	86.92 ± 0.56
L-CTL	86.40 ± 0.71	86.38 ± 0.75	86.00 ± 0.69	84.78 ± 0.39
G-ITL (top- b)	85.84 ± 0.54	85.92 ± 0.52	85.84 ± 0.54	85.55 ± 0.46
L-ITL (top- b)	85.44 ± 0.58	85.46 ± 0.54	85.44 ± 0.59	85.29 ± 0.36
G-CTL (top- b)	82.27 ± 0.67	82.27 ± 0.67	82.27 ± 0.67	82.27 ± 0.67
L-CTL (top- b)	80.73 ± 0.68	80.73 ± 0.68	80.73 ± 0.68	80.73 ± 0.68
BADGE	83.24 ± 0.60	83.24 ± 0.60	83.24 ± 0.60	83.24 ± 0.60
INFORMATIONDENSITY	79.24 ± 0.51	79.24 ± 0.51	79.24 ± 0.51	79.24 ± 0.51
RANDOM	82.49 ± 0.66	82.49 ± 0.66	82.49 ± 0.66	82.49 ± 0.66

Table 3: Magnitudes of γ_n for common kernels. The magnitudes hold under the assumption that \mathcal{X} is compact. Here, B_ν is the modified Bessel function. We take the magnitudes from Theorem 5 of Srinivas et al. (2009) and Remark 2 of Vakili et al. (2021). The notation $\tilde{O}(\cdot)$ subsumes log-factors. For $\nu = 1/2$, the Matérn kernel is equivalent to the Laplace kernel. For $\nu \rightarrow \infty$, the Matérn kernel is equivalent to the Gaussian kernel. The functions sampled from a Matérn kernel are $\lceil \nu \rceil - 1$ mean square differentiable.

Kernel	$k(\mathbf{x}, \mathbf{x}')$	γ_n
Linear	$\mathbf{x}^\top \mathbf{x}'$	$O(d \log(n))$
Gaussian	$\exp\left(-\frac{\ \mathbf{x}-\mathbf{x}'\ _2^2}{2h^2}\right)$	$\tilde{O}\left(\log^{d+1}(n)\right)$
Laplace	$\exp\left(-\frac{\ \mathbf{x}-\mathbf{x}'\ _1}{h}\right)$	$\tilde{O}\left(n^{\frac{d}{1+d}} \log^{\frac{1}{1+d}}(n)\right)$
Matérn	$\frac{2^{1-\nu}}{\Gamma(\nu)} \left(\frac{\sqrt{2\nu}\ \mathbf{x}-\mathbf{x}'\ _2}{h}\right)^\nu B_\nu\left(\frac{\sqrt{2\nu}\ \mathbf{x}-\mathbf{x}'\ _2}{h}\right)$	$\tilde{O}\left(n^{\frac{d}{2\nu+d}} \log^{\frac{2\nu}{2\nu+d}}(n)\right)$

numerically stable gradient embeddings) if ρ is too small, since this leads to numerical inaccuracies when computing the conditional embeddings. Apart from this, the effect of ρ is negligible.